

Characterization of the heparin binding site of tissue transglutaminase: its importance in the enzyme's cell surface targeting, matrix deposition and cell signalling

Zhuo Wang[†], Russell J. Collighan[†], Kamila Pytel[†], Daniel L. Rathbone, Xiaoling Li and Martin Griffin*
School of Life and Health Sciences, Aston University, Aston Triangle, Birmingham, B4 7ET UK.

*Corresponding author. Mailing address: School of Life and Health Sciences, Aston University, Aston Triangle, Birmingham, B4 7ET, UK. Phone: +44 (0)121 2043942. E-mail: m.griffin@aston.ac.uk

[†]These authors contributed equally to this study.

Running title: Heparan sulphate-related TG2 localization

Key words: tissue transglutaminase, heparan sulphate, extracellular matrix, trafficking, signalling

Capsule:

Background: TG2 is a multifunctional matrix protein and crosslinking enzyme.

Results: Identification and mutation of its heparan sulphate (HS) binding site blocks matrix deposition of TG2 as do inhibitors of syndecan shedding.

Conclusion: Coordinated binding to cell surface heparan sulphates facilitates TG2 cell surface trafficking and deposition into the ECM.

Significance: Blocking heparan sulphate binding provides an avenue for regulating the enzyme's pathological roles.

ABSTRACT

Tissue transglutaminase (TG2) is a multifunctional Ca²⁺ activated protein crosslinking enzyme secreted into the extracellular matrix (ECM), where it is involved in wound healing and scarring, tissue fibrosis, celiac disease and metastatic cancer. Extracellular TG2 can also facilitate cell adhesion important in wound healing through a non-transamidating mechanism via its association with fibronectin (FN), heparan sulphates (HS) and integrins. Regulating the mechanism how TG2 is translocated into the ECM therefore provides a strategy for modulating these physiological and pathological functions of the enzyme. Here, through molecular modelling and mutagenesis we have identified the HS binding site of TG2 ²⁰²KFLKNAGRDCSRSSPVYVGR²²². We demonstrate the requirement of this binding site for translocation of TG2 into the ECM through a mechanism involving cell surface shedding of HS. By synthesizing a peptide NPKFLKNAGRDCSRSS corresponding to the HS binding site within TG2, we also demonstrate how this mimicking peptide can in isolation compensate the RGD-induced loss of cell adhesion

on FN via binding to syndecan-4, leading to activation of PKC α , pFAK-397 and ERK1/2 and the subsequent formation of focal adhesions and actin cytoskeleton organization. A novel regulatory mechanism for TG2 translocation into the extracellular compartment that depends upon TG2 conformation and the binding of HS is proposed.

Abbreviations: TG2, Tissue transglutaminase; ECM, Extracellular matrix; FN, Fibronectin; HSPG, Heparan sulphate proteoglycans; HS, Heparan sulphate; MMPs, Matrix metalloproteinases; ERK1/2, Extracellular-signal regulated kinase1/2; HOB, Human osteoblasts; MEF, mouse embryonic fibroblast; gpITG, Guinea pig liver TG; tetracycline-inducible, tet-inducible; NS, Non-silencing; PMA, α -phorbol-12, 13-didecanoate; PKC α , Protein kinase C α ; FAK, focal adhesion kinase; CHO-K1, Chinese hamster ovary-K1; DMEM, Dulbecco's modified Eagle's medium; FBS, foetal bovine serum; α -Tub, α -Tubulin.

INTRODUCTION

Over-expression of the Ca^{2+} -activated tissue transglutaminase (TG2) is closely related to a wide range of pathological processes, such as wound healing and scarring, fibrosis, celiac disease multiple sclerosis and tumour metastasis (1,2). Under stress, cells over-express TG2, leading to enhanced externalization of the enzyme and the increased deposition of TG2 into the extracellular matrix (ECM). A huge amount of effort has been devoted to investigating the mechanism of TG2 secretion, but how it reaches the cell surface and is then translocated into the ECM is still unknown. Evidence suggests that TG2 is externalized via an unconventional secretion pathway, which may involve endosome binding (3) and association with the cell surface receptors and/or the ECM protein fibronectin (FN) (4). Once externalized, the enzyme can be deposited into the ECM where it forms a hetero-complex with FN and facilitates cell adhesion via an RGD-independent pathway, which during wound healing and matrix turnover can rescue RGD peptide-induced anoikis and subsequent loss of FN deposition through a syndecan-4/2 and $\alpha 5\beta 1$ integrin signalling pathway (5,6). However, in many pathological conditions the continuous deposition of TG2 into the matrix results in increased protein crosslinking leading to the onset of and progression of tissue fibrosis and scarring, celiac disease, tumour metastases and multiple sclerosis (1,7). Hence modulating the mechanism of TG2 translocation into the ECM provides an important basis for developing therapeutic strategies that are able to regulate its physiological and pathological functions.

Interestingly, cell surface heparan sulphate proteoglycans (HSPG), for which TG2 has a high affinity binding for, are also shed from the cell surface and can be deposited into the matrix where, like TG2, they are associated with a number of similar physiological and pathological conditions such as bone growth and development (8), wound healing and scarring (9), tumour progression (10) and angiogenesis (11). The HSPG family is composed of four major syndecans — syndecans 1-4, of which syndecan-1 and syndecan-4 are major resources for shedding into the ECM. By activation of cell surface matrix metalloproteinases (MMPs), in particular MMP-9 the HS loaded syndecan ectodomain can be cleaved and in turn deposited into ECM (12). The

aim of this study was firstly to identify the HS binding site within the TG2 molecule. To demonstrate the importance of this binding site in the translocation of TG2 into the ECM and to elucidate the mechanism(s) involved. Finally using a mimicking peptide resembling the HS binding domain on TG2 demonstrate directly the importance of this binding site in triggering syndecan-4-mediated intracellular signalling pathways that rescue cells from the stress-related RGD peptide-induced loss of cell adhesion.

EXPERIMENTAL PROCEDURES

Mammalian cell culture

Cell lines used in this study include human kidney epithelial cells HEK 293T/17 (ATCC CRL-11268) and mouse embryo fibroblasts NIH 3T3 (ATCC CRL-11268), Chinese hamster ovary cells CHO K1 (ATCC CCL-61) and the heparan sulphate deficient CHO-K1 derivative pgsD-677 (ATCC CRL-2244) (HS-mutant CHO), which were obtained from the American Type Culture Collection (ATCC, USA). Additionally, human osteoblasts (HOB) were kindly provided by Prof. S. Downes (University of Nottingham, Nottingham, UK). HEK 293T/17 cells, NIH 3T3 cells, HOB and opossum kidney (OK) cells were cultured in Dulbecco's modified Eagle's medium (DMEM) containing 10% (v/v) heat-inactivated foetal bovine serum (FBS), 2mM L-glutamine, nonessential amino acids, 100U/ml of penicillin and 100 $\mu\text{g}/\text{ml}$ of streptomycin. CHO-K1 and HS-mutant CHO cells were cultured in mixture F-12 (Ham) medium (Sigma-Aldrich, UK) supplemented with 10% (v/v) FBS. Tetracycline (tet)-inducible Swiss 3T3 cells transfected with wild type human TG2 were cultured and TG2 expression induced as previously documented (13). Cells were all maintained at 37°C in a 5% CO_2 humidified atmosphere.

Vector, antibodies, kits and reagents

The pcDNA3.1 vector and the DH5 α strain of *Escherichia coli* were purchased from Invitrogen (Paisley, UK). All restriction enzymes were obtained from New England Biolabs (Knowl Piece, UK). Wizard plus SV Minipreps DNA Purification system and Wizard SV gel and PCR Clean-up system were obtained from Promega (Southampton, UK). The endotoxin-free plasmid DNA maxi purification kit and the human and mouse syndecan-4 targeting siRNAs and their

universal negative control siRNA were obtained from Qiagen (Crawley, UK). KOD HOT Start DNA Polymerase was obtained from Merck Chemical Ltd. (Nottingham, UK), QuikChange II site directed mutagenesis kit was from Stratagene (Cheshire, UK). Cell transfection kits and reagents including Nucleofector kit R used for transfection of NIH 3T3 and OK cells was from Lonza Ltd. (Wokingham, Berkshire, UK). Guinea pig liver transglutaminase (gpITG2) was purified as described previously (14). The synthetic peptides **GRGDTP**, **GRADSP** and the PKC α specific inhibitor Go6976 were obtained from Calbiochem (UK). The P1 peptide (NPKFLKNAGRDCSRSS) and scrambled control peptide P1s (FNRADLKPRCGSSNKS), the peptide corresponding to the N-terminal end of TG2, AEELVLERCDLELE (P2) and the scrambled peptide EECRLAEELLEDVL (P2s), the GK21 peptide (GENPIYKSAVTTVVNPKYEGKRQIKIWFQN RRMKWKK) and its scrambled control peptide (GTAKINEPYSVTVPYGEKNKVRQIKIWFQN RRMKWKK) fused to the antennapedia third helix sequence (15) were synthesized by Peptide Protein Research, UK. Fibronectin and its purified 45 and 70kDa fragments, heparin, heparinase and chondroitinase were purchased from Sigma - Aldrich (UK). MMPs inhibitors were from Merck (UK). Antibodies used in this work are listed in **Table 1**.

Generation of the wild type TG2 and TG2 mutants

Wild type (wt) human (16) and C277S mutant (17) TG2 were amplified by PCR using primers TG2-F/TG2-R and cloned into the KpnI/NcoI sites of pcDNA3.1. The wt TG2 plasmid was then used to generate a set of TG2 mutants. These were constructed by either PCR in the case of Δ 1-15 TG2, or by using the QuikChange II site-directed mutagenesis kit (Stratagene, UK) for point mutations. Primers are shown in **Table 2**. The identity and proper arrangement of the TG2 mutants was verified by restriction analysis and nucleotide sequencing.

Transient transfection and expression of wild type TG2 and TG2 mutants in human HEK293T/17 cells, mouse NIH 3T3 cells and OK cells

HEK293T/17, NIH 3T3 and OK cells, which express very low levels of endogenous TG2, were

transiently transfected with wild type TG2 and the TG2 mutants. HEK293T/17 cells were transfected by the calcium phosphate procedure, while NIH 3T3 and OK cells were transfected by electroporation (Lonza Nucleofector, kit R). Transfected cells were grown for 48 h at 37 °C in a 5% CO₂ humidified atmosphere to allow expression prior to analysis.

Syndecan-4 silencing by siRNA transfection

The HP GenomeWide siRNA sequence targeting human syndecan-4 (SI00046816) (5) and siRNAs targeting mouse syndecan-4 (SI02691710, SI02714285, SI00201341 and SI02671543) and the non-silencing (NS) control siRNA were obtained from Qiagen (UK). The target sequences are non-homologues for any other syndecan types or cell surface receptors. The transfection was performed according to the manufacturer's protocol. Briefly, 3×10^5 cells/well HOB or tet-inducible Swiss 3T3 cells were seeded into 6-well plates for 24 h to reach 50-80% confluency. 150ng of siRNAs were used for each transfection by using HiPerFect transfection reagents. Following 30-48 h siRNA transfection, cells were used in cell adhesion assays (5).

Western blotting

Cells were lysed with cell lysate buffer (Santa Cruz, UK). Lysates containing 50 μ g of protein were dissolved in 2 \times Laemmli buffer (Sigma-Aldrich Ltd, Dorset, UK) and separated by SDS-PAGE. Western blotting was performed using specific primary antibodies as described above. Primary antibodies were detected using the appropriate secondary antibody conjugated to horse radish peroxidase. Detection was performed by using ECL chemiluminescence (Amersham ECLTM Western Blotting System, GE Healthcare, UK), where applicable α -tubulin (α -Tbl) was used for normalization of protein loadings using densitometry.

Biotinylation of cell surface proteins

Cell surface proteins were labelled by biotinylation as described previously (18). Briefly, cell monolayers were rinsed three times with ice-cold PBS pH 8.0 and labelled with 0.8mM sulfo-NHS-LC-biotin dissolved in PBS pH 8.0 at 4 °C for 20 min. Cells were then washed with 50mM Tris-HCl, pH 8.0 and lysed with 1% SDS at 4 °C in PBS, pH 8.0. Following denaturation at 95 °C, cell lysates were clarified by centrifugation at 14,000 \times g at 20 °C and 200 μ g of protein was

incubated overnight at 4°C with NeutrAvidin-Agarose resin. After washing three times with PBS pH 8.0, the biotin-labelled proteins were dissolved in 2× Laemmli buffer separated by SDS-PAGE and subjected to Western blotting. Cell surface levels of TG2 shown were normalised, using densitometry, to the total cell lysate values after the latter had been corrected for protein loading using α -tubulin. The wt cells were used as the 100% control. Value shown represents the mean values from 2 separate experiments unless stated otherwise.

Detection of TG2 in the ECM

Following transfection, cells were incubated for 24 h with 10% (v/v) serum, which was replaced with 1% (v/v) serum and TG2 expression and matrix deposition was allowed to proceed for a further 24 h, were then detached with 2mM EDTA in PBS, pH 7.4 and the ECM was extracted with 0.1% (w/v) deoxycholate in PBS, pH 7.4. The residual deoxycholate-insoluble ECM proteins were dissolved in 2× Laemmli buffer for further analysis by SDS-PAGE and Western blotting using Cub7402.

To detect the presence of TG2 in the ECM of TG2 transfected tet-inducible Swiss 3T3 cells, the cells were seeded into 6-well plates at the density of 3×10^5 cell/well. TG2 expression was induced by withdrawing tetracycline from the culture system (tet- cells), while cells cultured in the presence of tetracycline (tet+ cells) were used as the control. After induction of TG2 expression in the presence of certain treatments for 48 h, the cells were lifted with 2mM EDTA in PBS, pH 7.4 and lysed in cell lysis buffer and used as the cell lysate fractions. The ECM fractions were washed once and collected into 2× Laemmli buffer. Western blotting was performed to detect the target proteins by using specific antibodies. The treatments included: general MMP inhibitor GM6001, MMP-2/9 inhibitor, MMP-3 inhibitor and MMP-8 inhibitor at the concentration of 10 μ M, 10 μ g/ml heparin, 15mU/ml heparinase or chondroitinase, 0.5 μ M PMA or 5 μ M PKC α inhibitor Go6976. Matrix levels of TG2 shown were normalized to the total cell lysate values using densitometry after the latter was corrected for protein loading using α - tubulin. The wt cells or for the Swiss 3T3 cells the untreated cells, were used as the 100% control with values shown represented as a percentage of this. Values shown

represent the mean values from 2 separate experiments unless stated otherwise.

Dot blotting for ECM syndecan-4

To detect the presence of the shed syndecan-4 ectodomain in the ECM, modified dot blotting was applied. Briefly, tet-inducible 3T3 cells were seeded into 12-well plates at the density of 2×10^5 cells/ well and induced for TG2 expression for 48 h with the treatments (including PMA, Go6976, and the MMP-2/9 inhibitor) as described for TG2. The matrix fractions were then collected as described for the matrix TG2 and then dissolved into 2× Laemmli buffer. The ECM fractions containing equal amounts of protein were then loaded onto nitrocellulose membranes under vacuum using a dot blotter, washed and blocked with blocking buffer (5% (w/v) dried fat-free milk dissolved in TBS-Tween, pH 7.4) and the presence of syndecan-4 detected by immunoprobng with a specific antibody recognizing the ectodomain of syndecan-4.

Measurement of TG2 binding to FN by ELISA

Microtitre 96 well plates were coated with 50 μ l of 5 μ g/ml FN in 50mM Tris-HCl, pH 7.4 at 4°C overnight. The wells were blocked for 30 min with 3% BSA in PBS, pH 7.4 and washed twice with PBS-Tween, pH 7.4 and once with PBS, pH 7.4. Aliquots (100 μ l) of cell lysate containing 60 μ g protein were added to the FN-coated wells and incubated for 1 h at 37°C. After washing three times with PBS, pH 7.4, wells were blocked with 100 μ l 3% BSA in PBS, pH 7.4 for 30 min at room temperature and then incubated with 100 μ l Cub7402 (1:1000 dilution in blocking buffer) for 2 h at 37°C. After washing three times with PBS, pH 7.4, the wells were incubated with 100 μ l rabbit anti-mouse IgG-HRP conjugated antibody (1:1000 dilution in blocking buffer) for 2 h at 37°C. HRP was detected by the addition of 100 μ l of o-phenylenediamine substrate solution (Sigma Fast OPD, Sigma). Colour development was terminated by the addition of 50 μ l of 2.5M H₂SO₄ and absorbance at 490nm was measured. The amount of TG2/mutant TG2 binding to the FN was normalised between samples by using the densitometry values from Western blotting for the TG protein found in each of the cell lysates used. A-Tubulin was used to normalise for any differences in protein loading.

Inhibition of purified TG2 binding to FN by TG2-derived peptides

96-well Microtitre 96-well plates were coated overnight with either full length FN (5µg/ml) or its N-terminal fragments of 45kDa (54µg/ml) or 70kDa (45µg/ml) fragments which contain the TG2 binding site, in 50mM Tris-HCl, pH 7.4 as previously described (6,19). Wells were blocked with 3% BSA (w/v) in TBS pH 7.6. After three washes with PBS pH7.4, competitive peptides diluted in PBS, 2mM EDTA, pH 7.4 were added to the wells at concentrations from 10µM – 1mM and incubated for 1 h at room temperature. Wells were washed three times with PBS pH7.4 and purified human recombinant TG2 was added at a final concentration of 2µg/ml in the presence of the different concentrations of P2 or P2s peptides and incubated for 1 h at room temperature. After three washes with PBS pH7.4 bound TG2 was measured via ELISA as introduced above.

For the binding ability of TG2 when in either the fully closed or open conformation, gpITG (20mg/ml) was reduced by pre-incubation with 1mM DTT and then diluted (at least 20 fold) in PBS, pH 7.4. The reduced gpITG 20µg/ml was pre-incubated with 1mM GTP or GTP γ S (closed conformation) or TG2 site directed irreversible inhibitors R281 or R283 (extended conformation) at the concentration of 500µM (in the presence of 10mM Ca²⁺) at room temperature for 30 min. Treated enzymes were then incubated with the FN-coated wells at 37°C for 1 h as described in the Materials and Methods. 20µg/ml gpITG in 2mM EDTA in PBS, pH 7.4 was used as the positive control and 2mM EDTA in PBS, pH 7.4 was used as the negative control. TG2 bound to FN was detected via ELISA as described in the Materials and Methods. Values represent the mean \pm S.D. absorbance at 450nm from 3 experiments.

Binding of TG2 to heparin Sepharose

HEK cells, transiently transfected with wild-type and mutant TG2 were washed twice with ice cold PBS, pH 7.4, and lysed by the addition of 150 µl of 20mM Tris-HCl pH 7.4, 10mM EGTA, 2mM EDTA, 1mM NaF and 1mM Na₃VO₄. After clarification by centrifugation (300×g for 10 min), cell lysates were mixed with 450µl of 50mM Tris-HCl, 1mM EDTA, 1mM DTT, pH 7.5 and applied to a 5ml Heparin Sepharose column (GE Healthcare) equilibrated in 50mM Tris-HCl, 1mM EDTA, 1mM DTT pH 7.5 (buffer) at a flow rate of 1ml/min. For the analysis of GTP-bound TG2 (closed conformation), lysates were pre-incubated

for 1 h at room temperature with 0.5mM GTP in 50mM Tris-HCl, 2mM MgCl₂, 1mM EDTA, 1mM DTT pH 7.5. For the analysis of inhibitor-reacted TG2 (open conformation), lysates were incubated with 0.5mM of irreversible inhibitor R281 (20) and 10mM CaCl₂. The column was washed with 25ml of buffer and protein was eluted with a linear gradient of increasing NaCl concentration (0-1M) in buffer. Fractions were assayed for TG2 activity and analysed for the presence of TG2 antigen by SDS-PAGE and Western blotting using CUB7402.

Measurement of TG activity in cell lysates and heparin Sepharose fractions

TG activity in column fractions was measured by biotin X-cadaverine incorporation into N,N'-dimethylcasein as described previously (21). After coating the wells with 100µl of 10mg/ml N,N'-dimethylcasein in 50mM Tris-HCl, pH 8.0, plates were washed with TBS-Tween, pH 7.6 and TBS, pH 7.6, and 50µl of column flow-through as well as each eluted fraction was added into the coated wells. Additionally 50µl of 100mM Tris-HCl pH 8.0, 0.25mM biotin X-cadaverine, 10mM DTT, 20mM CaCl₂ (or 5mM EDTA as control) was added into each well. The reaction was allowed to proceed for 1 h at 37°C. The plate was then washed once with TBS-Tween, pH 7.6 and TBS, pH 7.6 before being blocked with 100µl of 3% (w/v) BSA in TBS, pH 7.6, for 30 min at 37°C. After another wash, biotin X-cadaverine incorporation into N,N'-dimethylcasein was detected by incubation for 1 h at 37°C with 100µl Extravidin-peroxidase (Sigma-Aldrich, UK) diluted 1:2000 in 3% (w/v) BSA in TBS, pH 7.6. After another set of washes, TG2 activity was measured using Sigma Fast OPD, tablets dissolved in 20ml of distilled H₂O. The colour was developed by adding 2.5M H₂SO₄ and the absorbance at 490nm measured using a microplate reader.

For cell lysates the incorporation of biotin-X-cadaverine into FN as described previously was used (21). Briefly, wells of 96-well plate were coated with 5 µg/ml of FN in a 50mM Tris-HCl, pH 7.4 and incubated overnight at 4°C. After washing with 50mM Tris-HCl, pH 7.4, wells were blocked with 3% (w/v) BSA in 50mM Tris-HCl pH 7.4 for 30 min at 37°C. Enzyme reactions contained 50µg of cell lysate protein in 50mM Tris-HCl pH 7.4 buffer containing 5mM CaCl₂ (or 5mM EDTA as control), 10mM DTT, 0.132mM biotin X-cadaverine each done in triplicate.

Reactions were allowed to proceed for 2 h at 37°C. Plates were then processed as described above.

Cell adhesion assays

The cell adhesion assay was carried out as previously described (18). Briefly, 96-well plastic tissue culture plates were coated with 5µg/ml FN in 50mM Tris-HCl, pH 7.4 at 4°C overnight, after washing three times with 100µl of 50mM Tris-HCl, pH7.4, gpITG (20µg/ml) in 2mM EDTA in PBS, pH 7.4 was added to the wells for 1 h at 37°C and the wells were washed three times with 50mM Tris-HCl, pH7.4. Serum-starved (for 16 h) HOB cells with different treatments as introduced below in serum-free medium were detached by trypsinization and then treated with trypsin inhibitor. Cells were washed three times with serum free medium and seeded onto either FN or TG-FN matrix for 20-40 min. Peptides P1 or scrambled P1 (P1s), were added at concentrations between 100µg/ml and 300µg/ml. To determine the RGD-independent cell adhesion, assays were performed by incubating cells with either RGD or RAD peptide (100µg/ml) unless stated otherwise in the presence of the P1 or P1s peptides for 20 min prior to seeding of the cells. Attached cells were washed once with PBS, pH 7.4 and then fixed with 3.7% paraformaldehyde, further permeabilized with 0.1% (v/v) Triton-X in PBS, and co-stained with May-Grunwald and Giemsa stains as described previously (5). Images of stained cells from non-overlapping fields of view were photographed at 20× magnification and analyzed using the imaging analysis program Scion Image (National Institute of Health). Cell attachment and spreading were quantified, and the number of cells per image was assessed as described previously (19). Cell attachment on FN without peptide was considered as the control value for all the experiments unless stated otherwise. The mean number of attached cells from at least three wells was calculated and that of the control was considered as 100%. The mean number of attached cells (cell attachment) for each sample was then expressed as the percentage of cell attachment on FN. The mean percentage of attached cells that are spread (cell spreading) for each sample was determined separately, and the mean percentage of spread cells on FN control was expressed as 100%. The mean percentage of spread cells for each sample was then normalised against that of FN control. Cell attachment on FN

without the RGD peptide was considered as the control value for most of the experiments unless stated otherwise. The mean number of attached cells from three wells was calculated and that of the control was considered as 100%. The mean number of attached cells (cell attachment) for each sample was then expressed as the percentage of cell attachment on FN. The mean percentage of attached cells that are spread (cell spreading) for each sample was determined separately, and the mean percentage of spread cells on the FN control was expressed as 100%. The mean percentage of spread cells for each sample was then normalised against that of FN control. Cell pre-treatments included: PKCα inhibitor Go6976 (5µM) or GK21 peptide (8µM, which blocks the interaction between PKCα and the intracellular domain of β1 integrins) for 1 h in serum-free medium prior to cell detachment; heparinase (15mU/ml) or chondroitinase (15mU/ml) to cells in suspension in serum free medium for 1 h; or α5β1 integrin blocking antibody NKI-SAM-1 and its isotype control antibody (20µg/ml) in serum free medium for 1 h. For the detection of the signalling molecules via Western blotting, the cell adhesion assay was performed in 60mm Petri dishes and cells were collected into cell lysis buffer (Santa Cruz, UK) as described previously and pre-cleared by centrifugation at 300×g for 10 min. Western blotting was performed with specific anti-p-397 FAK or p-ERK1/2 antibodies. Membranes were stripped (19) and total FAK and ERK1/2 detected using anti- FAK and anti- ERK1/2 antibodies as listed in Table 2, while α-tubulin was used as an equal loading standard (5).

Fluorescence Staining

Cell adhesion on FN matrix in the presence of either the P1 or the P1s peptide (100µg/ml) was performed as described above. Cells were seeded in 8-well glass chamber slides (8×10^4 cells/well) previously coated with FN and allowed to attach and spread for 20-40 min. Cells were fixed and permeabilized as described above and then blocked with 3% BSA in PBS, pH 7.4, (the blocking buffer) for 30 min. For the actin stress fibre staining, the cells were incubated with FITC-labelled Phalloidin (20µg/ml) in blocking buffer. For the focal contact staining in HOB cells, after treatment with blocking buffer, the cells were incubated with anti-Vinculin antibody (1:100 dilution) followed by anti-mouse IgG-TRITC at

37°C for 2 h/incubation. Slides were mounted with Vectashield mountant (Vector Laboratories) and examined via confocal microscopy (5).

For the FITC-cadaverine incorporation *in situ* assay, tet-inducible Swiss 3T3 cells were seeded into 8-well chambers at the density of 7×10^4 cells/well. Together with the withdrawal of the tetracycline, the cells were treated with PKC α inhibitor Go6976, MMP-2/9 inhibitor, MMP-8 inhibitor, heparin and heparinase as described above. After 48 h induction of TG2 expression, fresh medium with 0.5mM FITC-cadaverine (with or without the treatment) was incubated with the cells at 37°C for 1 h. The wound was introduced into the mono-cell layer using a sterile plastic pipette tip and the cells were incubated for another 1 h as described previously (22). After washing three times with PBS, pH 7.4, the cells were fixed with methanol at -20°C for 10 min and then mounted in Vectorshield mountant medium and the fluorescence signal detected by fluorescence microscopy.

Co-immunoprecipitation assay for the interaction between TG2 and syndecan-4

Tet-inducible Swiss 3T3 cells (5×10^5 cells/well) were seeded into 6-well plate and TG2 expression was induced by withdrawing tetracycline from the cell culture system. 200 μ g/ml of P1 or P1s peptide was used together with the TG2 induction. The cell lysates were collected into the co-IP buffer and co-IP was performed to detect the interaction between TG2 and syndecan-4 as introduced previously [14]. Briefly, 0.5 μ g of anti-syndecan-4 antibody was used to pull down the syndecan-4-immunocomplex from the precleared cell lysates and Western blotting was carried on to detect the presence of TG2 in the immunocomplex by using specific anti-TG2 antibody Cub7402. The non-induced Swiss 3T3 cells with the undetectable TG2 expression were used as the negative control.

Solid binding assay for the P1 peptide binding to syndecans

To detect the binding specificity of P1 peptide toward syndecan-4 and syndecan-2, ELISA plates were coated with P1 peptide at the concentration of 1 μ g/ml in Na₂CO₃ solution pH 9.6 at 4°C for overnight. The wells were blocked with 3% BSA in PBS, pH 7.4 after washing with 50mM Tris-HCl, pH 7.4. 2 μ g/ml recombinant human syndecan-4 or syndecan-2 (with the his-tag) in 50mM Tris-HCl, pH 7.4 was incubated with the

wells at 37°C for 1 h. The presence of syndecan-4 or syndecan-2 bound to the peptide-coated wells was detected by using anti-His tag antibody and anti-mouse secondary. The signals were detected by using OPD substrate and the absorbance was measured at 490nm.

Docking studies

The crystal structures 1KV3 and 2Q3Z were downloaded as pdb files from the Protein Data Bank (<http://www.rcsb.org/>) and opened in the software CAChe WorkSystem Pro version 7.5.0.85 (Fujitsu Ltd). Hydrogens were added and waters and ions were deleted. The hydrogen atom positions were relaxed by conducting a MM2 geometry optimisation for each structure where all the non-hydrogen atom positions were locked. For the HS1 site, docking sites were defined by selecting all the amino acid residues within either 5 Å or 8 Å of residues K600, R601 and K602. For the HS2 site, docking sites were defined by selecting all the amino acid residues within either 5 Å or 8 Å of residues K202, K205, R209, R213 and R222. Both crystal structures contained missing residues but these were far enough away from the defined docking sites such that their absence would not interfere with the docking studies. Using the same software, three ligand structures (a dimer, a pentamer and a hexamer) were defined by taking residues 2-3, 2-6 and 2-7 respectively from the glycosaminoglycan structure 1HPN.pdb. Using the Project Leader module and the Active Site docking component of the same software, the three ligands were each docked three times into the defined docking sites of both proteins using the flexible ligand and flexible active site side chain options. Other parameters and options included: Use Amber van der Waals; population size 50; maximum generations 3000; crossover Rate 0.8; mutation Rate 0.2; elitism number 5; local search rate 0.06; maximum iterations local search 300.

Data analysis

Results shown are the mean \pm S.D. unless otherwise stated. The differences between data calculated was undertaken by Student's t-test and indicated as significant when the $p < 0.05$.

RESULTS

Identification of putative heparin-binding motifs in TG2

HS-binding motifs may be composed of basic amino acid-containing sequences, such as XBBXB or XBBBXXB, where B is a basic amino acid whose side chain is exposed on the protein surface and X is a neutral or hydrophobic amino acid, whose side chain is directed towards the protein interior (23). Examination of the primary amino acid sequence of TG2 for these linear consensus HS binding motifs revealed one such sequence ²⁶¹LRRWKN²⁶⁶ close to the active site of TG2 (**Figure 1A**) (24). Examination of the crystal structure of TG2 (1KV3) shows that ²⁶¹LRRWKN²⁶⁶ is part of an alpha helix, whereas the XBBXB consensus must be in a β -sheet in order for the basic residues to face the same direction. A common structural theme of linear HS binding motifs is that there are two basic residues approximately 20Å apart to accommodate a pentasaccharide, facing in opposite directions on an alpha helix (25). Since ²⁶¹LRRWKN²⁶⁶ is too short to satisfy this requirement it is unlikely to be able to bind HS and so was ruled out. The three dimensional arrangement of basic amino acid residues is likely to be more important than linear clustering, such that many HS binding motifs can also be comprised of sequence-distant basic amino acid residues (26). Examination of the crystal structure of TG2 revealed two likely candidate motifs, ⁵⁹⁰KIRILGEPKQKRK⁶⁰² (HS1) which is located at the tip of C-terminal β barrel 2 and another comprised of ²⁰²KFLKNAGRDCSRSSPVYVGR²²² with K387 (HS2), forming a shallow pocket lined with basic residues (**Figure 1A-C**). Importantly both of these sites are likely to allow simultaneous binding of fibronectin (**Figure 1A**) as previously described (6,19,27).

A heparin-derived oligosaccharide docks into a characteristic heparin binding pocket in TG2

The HS1 and HS2 regions were docked with heparin derived oligosaccharides. An iduronic acid-2-sulphate-glucosamine-2, 6-disulphate disaccharide, which is the most common repeating unit of heparin This docked better with the HS2 region than the HS1 region of the closed form of TG2 (1KV3) although both sites docked well .A pentasaccharide and a hexasaccharide with the same repeating units bound with a similar enthalpy to both the HS2 and HS1 site (see **Figure 1D** and **E**). The same oligosaccharides failed to dock as successfully with the open conformation of TG2

(2Q3Z) at both the HS1 and HS2 sites although slight preference was shown for the HS1 site (**Supplementary Table 1**).

Expression of the FN and HSPG TG2 mutants in mammalian cell systems

Mutant TG2 enzymes for the binding of FN (D94A, D97A), the N-terminal deletion (Δ 1-15) and HS mutants HS1 (K600A, R601A, K602A) and HS2 (K205A, R209A) were generated by mutagenesis of plasmid pcDNA3.1-TG2. Mutants were confirmed by nucleotide sequencing and transfected into HEK293T/17 and NIH 3T3 cells to assess expression. All mutants were expressed in both cell types (**Figure 2A** and **2D**) and by Western blotting showed bands of the expected molecular weight (**Figure 2A** and **2D**) although at slightly different levels, with the Δ 1-15 TG2 mutant showing significantly less expression in both cell types when compared to the wt cells (**Figures 2B, C, E** and **F**). Comparable transamidating activities were found with all mutants when normalised to TG2 protein (**Figure 2C** and **2F**) apart from the Δ 1-15 TG2 mutant which was significantly lower (approx 50%) than the wt enzyme in HEK293T/17 cells but still present, suggesting no evidence for gross misfolding.

The high affinity heparin binding site of TG2 is located in the catalytic core domain

TG2 binds to heparin Sepharose with high affinity, and has been used for its purification. The binding strength of TG2 and mutants HS1 and HS2, expressed in HEK 293T/17 cells, to heparin Sepharose was determined by elution with an increasing salt gradient (**Figure 3A**). TG2 was eluted over a very broad peak ranging from 100mM NaCl to 500mM NaCl with optimum elution at 330mM NaCl. To rule out that the observed low affinity binding was due to denatured TG2, the transglutaminase activity of eluted fractions was determined and this showed that specific activity did not differ significantly between fractions (**Supplementary Figure 1**).

Mutant HS1 bound heparin identically to TG2, with low and high affinity, whereas HS2 lost its high affinity binding to heparin, with a large percentage of the mutant showing no binding to the heparin column and the remainder showing low affinity binding, eluting at a NaCl concentration of 60mM (**Figure 3A**), suggesting that residues K205 and R209 contribute to the high

affinity binding to heparin. Since mutant HS1 had a higher net charge reduction than HS2, this alteration in HS2 binding was not simply due to electrostatic interaction. Comparable studies with the D94A, D97A FN mutant showed this mutant had a comparable elution profile to the wt enzyme. However, the Δ 1-15 TG2 FN binding mutant showed only a low affinity binding to the heparin column with the major peak eluting at around 250mM NaCl.

High affinity heparin binding is dependent on TG2 conformation

Since TG2 can adopt two extremes of conformation in the presence or absence of GTP, the effect of GTP binding on the association of TG2 to heparin was also investigated (**Figure 3A**). In the presence of GTP, which results in a compact globular conformation, all of the TG2 bound with high affinity to heparin with the major peak eluting at about 330mM NaCl. In contrast, after reaction with the irreversible peptidic inhibitor R281 (20) or mutation of the active site Cys²⁷⁷ to Ser, which restricts the conformation to an extended form, the TG2 bound to heparin with lower affinity with the major peak eluting at 250mM NaCl. Since the GTP-bound globular form of TG2 bound to heparin with high affinity whilst the extended R281-bound form still retained an affinity greater than that of the HS2 mutant, this suggests that the loss of high affinity binding of HS2 is not solely due to an altered conformation. Hence, TG2 residues K205 and R209 are very likely to be directly involved in high affinity heparin binding.

Studies with the HS2 peptide NPKFLKNAGRDCSRRSS (P1)

Our previous studies (6,19,27) indicated that TG2, when regulating cell adhesion via syndecans, interacted directly with syndecan-4, but not syndecan-2 which was activated indirectly via PKC α . We therefore tested the binding specificity of the TG2 HS2 region toward these two syndecans. A peptide ²⁰⁰NPKFLKNAGRDCSRRSS²¹⁶ (P1), which mimics the heparin binding domain in TG2, was synthesized. This peptide was chosen for its potential to fold correctly and the hydrophobic C-terminal sequence PVYVGR, which may affect solubility, was excluded. A solid binding assay was undertaken to study the binding ability of this peptide toward syndecan-4 and syndecan-2, in

which his-tagged recombinant human syndecan-4 or syndecan-2 was assessed for their binding to the immobilised P1 peptide and then detected by using anti-his tag antibody. As shown in **Figure 3B**, strong preference was shown for syndecan-4 binding to the P1 peptide when compared to the binding of syndecan-2, suggesting that the binding specificity of the P1 peptide towards syndecan-4 confirms our previous findings that TG2 binds preferentially to the heparan sulphate chains on the cell surface syndecan-4 and not syndecan-2 (6). Using immunoprecipitation, we further tested the competitive effect of the P1 peptide for the interaction between syndecan-4 and TG2. To confirm this specificity and to rule out any potential toxicity of the P1 peptide to the cells, a scrambled peptide (P1s, FNRADLKPRCGSSNKSR) was also used. **Figure 3C** shows that the immunoprecipitation of TG2 with anti-syndecan-4 antibody was reduced around 50% in the presence of the P1 peptide, but no effect was found with the scrambled analogue, thus confirming the specificity of the P1 peptide for syndecan-4.

Using cell studies, we then investigated if the peptide P1 can mimic TG2 in cell adhesion studies and as such can either substitute for or abolish the TG2-mediated compensation of the RGD-mediated loss of cell adhesion. In our earlier studies using both HOB and mouse embryonic fibroblast (MEF) cells, it was shown that extracellular TG2 bound to matrix FN could compensate for the loss of integrin-mediated cell adhesion in the presence of RGD peptides in a process requiring cell surface syndecan-4, but not its transamidase activity (27). Since direct interaction of TG2 with syndecan-4 is essential for this process, the HSPG binding properties of TG2 are therefore critical. The P1 peptide was tested for its ability to compensate the RGD-induced loss of cell adhesion on FN in HOB cells. At a peptide concentration between 0.01-200 μ g/ml, significant compensation started as low as 5-10 μ g/ml with maximum compensation achieved between 50-100 μ g/ml (**Figure 4A**). We then investigated whether the P1 peptide, when used at a concentration of 100 μ g/ml, could compete for the binding of syndecan-4 and abrogate the compensatory effects of TG-FN, when the cells were plated onto the TG-FN matrix in the presence of the RGD peptide. **Figure 4B** shows that P1

peptide only has a small, but not significant dose-dependent negative effect on the attachment and spreading of HOB cells on TG-FN in the presence of the RGD peptide, whereas the scrambled control peptide P1s had almost no effect. This suggests that even though the peptide may compete for TG2 for the syndecan-4 binding site its ability to mimic TG2 in compensating RGD-induced loss of cell adhesion means no large changes in cell adhesion are likely to be observed. Neither peptide significantly affected the binding of cells to FN alone when used at similar concentrations of 100-300 μ g/ml, although a small (approx 10%) but significant enhancement of adhesion was found for P1 peptide when compared to the P1s peptide (**Figure 4B**). Importantly, the TG2 mimicking P1 peptide was able to restore actin cytoskeleton formation and focal adhesion assembly, which was disrupted with the RGD peptide (**Figure 5A and B**), while the scrambled analogue FNRADLKPRCGSSNKSR (P1s) showed no effect on either of these.

P1 peptide acts via binding and activation of syndecan -4-mediated cell signalling

Further confirmation that the P1 peptide can act like extracellular TG2 in compensating α 5 β 1 integrin loss (6) of cell adhesion was shown by pre-incubated cells with the P1 peptide prior to incubation with the α 5 β 1 integrin blocking antibody (NKI-SAM-1). The P1 peptide led to a significant increase in cell adhesion in the presence of the inactivating antibody when compared to the control cells incubated with the antibody in the presence and absence of the P1 scrambled peptide (**Figure 6A**).

To test the importance of cell surface HS in the binding of P1 peptide, HOB cells were pre-treated with heparinase or chondroitinase prior to the cell adhesion assay. Treatment with heparinase, but not chondroitinase, abolished the compensatory effect of the P1 peptide on the RGD-induced loss of cell adhesion (**Figure 6B**). To confirm that the P1 peptide is binding to cell surface syndecan-4 molecules, HOB cells were treated with syndecan-4 siRNA and scrambled control siRNA as previously documented (5). As previously found (5) treatment of HOB cells with syndecan-4 siRNA led to a around 50% reduction in protein expression (**Supplementary Figure 2A**) without affecting either syndecan-2 or β 1 integrin

expression, another two major players in the TG-FN complex-mediated signalling pathway (18).

This loss in expression of syndecan-4 led to a comparable but significant reduction in the compensatory effect for the P1 peptide on the RGD-induced loss of cell adhesion (**Figure 7A**). The scrambled siRNA had no significant effect on either expression or cell adhesion, further confirming the essential role of syndecan-4 in the P1 peptide-related cell adhesion process.

Our next step was to demonstrate the activation of protein kinase C α (PKC α) in the signalling effects mediated by the P1 peptide. The PKC α inhibitor Go6976 and the GK21 peptide (which is reported to compete with the PKC α binding site on β 1 integrin (15) both inhibit PKC α activation events leading to a significant loss of the compensatory effect of the P1 peptide on the RGD-induced loss of cell adhesion (**Figure 7B and C**), strongly suggesting that the P1 peptide is acting in a comparable signalling manner to that of TG2. To confirm our observations that the P1 peptide is inducing intracellular signalling pathways comparable to the TG-FN matrix, we looked at the activation of focal adhesion kinase (FAK) by phosphorylation at Tyrosine 397 (**Figure 8A and 8B**) and phosphorylation of extracellular-signal regulated kinase1/2 (ERK1/2) (**Figure 8C and 8D**). In each case, in the presence of RGD and P1 peptide the compensation of the RGD-induced loss of adhesion was paralleled by a significantly greater phosphorylation of p-FAK³⁹⁷ than that found with the P1s peptide, thus confirming the ability of the P1 peptide to restore focal adhesion assembly and activation of p-ERK1/2 (**Figure 8A-D**).

The N-terminus of TG2 is involved in FN binding

The Δ 1-15 and D94A, D97A TG2 mutants were assessed for their ability to bind to FN in a solid phase binding assay utilising purified FN and clarified lysates from HEK 293T/17 cells transfected with the different mutants. The D94A, D97A mutant described previously (28) demonstrated significantly less binding (approx 50%) compared to wild type TG2, whereas the Δ 1-15 deletion mutant previously described (28) had approximately 60% less ($p < 0.05$) binding capacity of the wild type (**Figure 8E**). A competitive peptide corresponding to the N-terminal deletion site of TG2

²AEELVLERCDLELE¹⁵ (P2) (TG2 undergoes N terminal post-translational modification of the N-terminal methionine) was tested for its ability to inhibit wild type TG2 binding to FN and the smaller TG2 binding N-terminal FN fragments of 45 and 70kDa in a solid binding assay. The P2 peptide resulted in a moderate but significant inhibition of binding to FN and its smaller fragments at higher concentrations (500µM-1mM) of the peptide not shown with the scrambled P2s peptide (**Figure 8F** and **8G**), suggesting that the N-terminal residues 1-15 of TG2 may be important for FN binding, in addition to the published D94A, D97A site. However, the limited inhibition seen with this peptide suggests that the FN binding site around the N-terminal site of TG2 may be more complex and that a larger structural unit than that described previously (28) may be involved in FN binding.

HS binding is required for ECM localisation of TG2

Since TG2 has been shown to have a high affinity binding for heparan sulphates (29), we investigated the ability of the FN and HS-binding mutants to be secreted to the cell surface and/or deposited into the ECM. Using transfected NIH 3T3 fibroblasts, the cellular localisation of the D94A, D97A FN mutant, the Δ1-15 mutant and the HS1 and HS2 TG2 mutants were tested for their presence at the cell surface using the cell surface biotinylation assay. For detecting the presence of these mutant TG2s in the ECM, transfected NIH 3T3 cells were used, which actively deposit ECM. The TG2 Δ1-15 mutant was not detected on the cell surface of the NIH3T3 cells (**Figure 9A**) whereas the HS2 mutant was detected but in very reduced amounts compared to the wild-type TG2. The levels of the FN mutant D94A, D97A and the HS1 mutant were found at comparable levels on the cell surface to that shown for the wild-type TG2 (**Figure 9A**). A comparable picture was observed for the presence of the TG2 wt and mutants in the ECM of NIH 3T3 cells apart for the HS2 mutant and the Δ1-15 mutant which were barely or not detectable respectively within the matrix (**Figure 9B**).

Cellular localisation of TG2 in CHO wt and CHO-HS-M cells

To confirm the importance of cell surface HS in the cell surface distribution of TG2, the HS deficient Chinese hamster ovary-K1 (CHO-K1)

cells derivative pgsD-677 were compared to wt CHO-K1 cells with respect to their distribution of TG2 at the cell surface (**Figure 9C** and **9D**), which clearly demonstrates that the amount of TG2 found at the cell surface in the CHO mutant cells is considerably reduced when compared to the wt cells.

The involvement of syndecan shedding in deposition of matrix TG2

We next determined whether cell surface syndecan shedding may be a possible mechanism for translocating HS-bound TG2 into the extracellular matrix. Since MMPs are reported to be involved in the shedding of cell surface HS into the ECM (12), a general MMP inhibitor GM6001 was first used to treat TG2 transfected Swiss 3T3 cells. TG2 expression can be induced in these cells via the tet-inducible promoter and is externalised and deposited into the matrix in large amounts (27). Following induction of TG2 by withdrawal of tetracycline (tet-) from the cell culture system, the matrix deposited TG2 is detectable after a 48 h induction (**Figure 10A**). In the presence of the MMP inhibitor GM6001 (10µM) the matrix deposited TG2 was very much reduced although expression of TG2 was not affected. The negative control treatment did not show any effect on TG2 expression and deposition (**Figure 10A**). To clarify which member(s) of the MMP family members are involved in the TG2 deposition, specific MMP inhibitors against MMP-2/9, MMP-3, MMP-8 were used. As shown in **Figure 10B**, the MMP-2/9 inhibitor reduced the matrix TG2 deposition by around 50%, which was not apparent in the other MMP inhibitor treated cells. This suggests that the MMP-2/9 inhibitors which are the major MMP members participating in wound healing and HS shedding (12,30), are also involved in ECM TG2 deposition. Different treatments (12,31) known to affect HS shedding were then used in the tet-inducible 3T3 cells. **Figure 10C** shows that PMA, an enhancer for HS shedding (31), slightly increased the amount of matrix TG2, while the PKCα inhibitor Go6976 (an inhibitor for HS shedding (12)) blocked deposition of TG2 into the ECM. Heparin (at the concentration of 10µg/ml), a known protector of MMP-dependent HS shedding (32), reduced the presence of TG2 in the matrix, while heparinase (which digests the cell surface HS chains) completely inhibited matrix TG2 deposition. In

contrast chondroitinase did not show any effect on matrix TG2 deposition (**Figure 10C**). By using syndecan-4 siRNA targeting mouse syndecan-4, the expression of syndecan-4 was reduced to around 50% compared to the non silencing (NS) control (**Supplementary Figure 2B**), which led to a comparable reduction of ECM deposited TG2 deposition (**Figure 11A**). To confirm that comparable levels of syndecan-4 to that found for TG2 are found in the ECM following treatment of cells with the same key modulators of syndecan shedding. The matrix of the treated cells was collected and immunoprobed for the presence of syndecan-4. As shown for TG2, PMA, an enhancer of syndecan shedding, increased the amount of syndecan-4 present in the ECM, while the inhibitors of shedding PKC α inhibitor Go6976 and the inhibitor of MMP-2/9 reduced the amount of syndecan-4 present in the ECM (**Figure 11B**). To assess whether HS shedding may contribute to the increased TG2 activity found in the matrix following wounding (22,33), fluorescence staining using FITC-cadaverine as a measure of TG2 *in situ* activity was used. After wounding the tet-inducible 3T3 cells in a scratch assay, cells were incubated for a 1 h period with FITC-cadaverine. As shown in **Figure 12**, the PKC α inhibitor Go6976, MMP-2/9 inhibitor, heparin and heparinase treatments and the peptidic TG2 irreversible inhibitor R281 all reduced the presence of *in situ* TG2 activity found at the edge of the wound when compared to the non-treated control. This reduction was not seen with either MMP-8 or chondroitinase treatment, thus confirming the importance of syndecan shedding in delivering increased TG2 activity to the matrix after wounding.

DISCUSSION

Identifying and subsequently being able to regulate the mechanism of TG2 translocation into the ECM provides a novel strategy for modulating the pathological functions of the enzyme. Earlier studies suggest that cell surface HSPGs might be important in the trafficking of TG2 onto the cell surface (29). However, evidence for a HS binding site on TG2 has not been proven. We therefore identified the HS binding site(s) within TG2 by using a combination of amino acid sequence analysis for known HS-binding motifs and by analysis of the available crystal structures of TG2.

Two potential binding sites were identified (HS1 and HS2), which were docked with heparin derived oligosaccharides consisting of an iduronic acid-2-sulphate-glucosamine-2, 6-disulphate disaccharide, which is the most common repeating unit of heparin. Both the HS1 and HS2 sites docked well with all the oligosaccharides when TG2 was in its closed conformation although the HS2 site was the preferred site. In comparison, neither site docked well when the open conformation of TG2 was used, although slightly better docking was observed with the HS1 site. As a consequence, of these results it was decided to subject both sites to site directed mutagenesis of the key surface-exposed basic residues. By using a heparin affinity chromatography column we showed that the HS2 site, comprising residues ²⁰²KFLKNAGRDCSRRSSPVYVGR²²², was required for high affinity binding to heparin whereas mutation of the HS1 site showed no difference in binding to that of the wt enzyme TG2 can adopt two extremes of conformation: a compact conformation when guanine nucleotides are bound and an extended catalytically active conformation when guanine nucleotides are displaced by calcium binding (33,34). Our docking studies for both the HS1 and HS2 site predicted a good interaction between the HS-binding site of the compact form of TG2 and heparin oligosaccharides, but the extended conformation in particular for the HS2 site did not produce comparable interactions, suggesting that binding affinities for TG2 and heparin might be conformation-dependent. Using heparin affinity chromatography, we confirmed that GTP-bound TG2 (compact form) binds strongly to heparin (eluted at 330mM NaCl), whereas R281-reacted TG2 (extended form) binds weaker (eluted at 250mM NaCl). The C277S mutant, known to be in the extended conformation, binds to heparin with similar affinity to the R281-reacted TG2. Hence under normal physiological salt conditions the binding affinity of TG2 for cell surface HS is likely to be conformation dependent.

Mutation of two surface exposed basic residues (K202 and R205) in the HS2 site did not affect TG2 activity or FN binding, however this mutant only bound very weakly to the heparin column, with one large pool of mutant eluting at 60mM NaCl and another failing to bind at all. Both of these pools of eluted enzyme showed full TG

activity which could be inhibited by GTP indicating that the HS2 mutant is still able to bind to this nucleotide (**Supplementary Figure 1**). Hence the affinity of the K205, R209 mutant for heparin is significantly lower than that of either GTP-bound or R281-reacted wild type TG2 and it is likely that little binding would occur at physiological ionic strength. In support of this both HEK 293T/13 and NIH 3T3 cells expressing the HS2 mutant showed much reduced amounts of the HS2 mutant on the cell surface and it was found to be barely present in the ECM of the NIH 3T3 cells. In view of a very recent paper (35) indicating that the N-terminal β -sandwich domain of TG2 is essential for TG2 secretion to the cell surface in kidney OK epithelial cells, we also measured the amount of the cell surface HS2 mutant and matrix associated HS2 in these same cells (**Supplementary Figure 3**). Again despite a good expression level of this mutant, there was little HS2 mutant present at the cell surface, while the enzyme was absent in the matrix, thus agreeing with our data for the HEK and the HS2 mutant transfected NIH 3T3 cells. Support for the importance of HS in the trafficking of TG2 to the cell surface was obtained using TG2 expressing HS-mutant CHO cells (which are unable to synthesize HS, but are still able to maintain the presence of the core proteins of the proteoglycans in the cell membrane (36)). A multiple alignment of TG peptide sequences, including TG2 from different species and human TG isoforms (**Supplementary Figure 4**) shows that the high affinity heparin binding domain is conserved amongst TG2 enzymes, but is absent from other isoforms with residues corresponding to human TG2 positions 202, 205, 213 and 222 conserved as basic residues amongst all the TG2 sequences analysed.

Syndecan shedding is found in many physiological and pathological situations, where upregulation of TG2 expression also occurs e.g. during wound healing, in cancer migration and in bone differentiation and mineralisation (9,37). To study the involvement of syndecan shedding in the trafficking of TG2 into the matrix, we used the well characterised stably transfected Swiss 3T3 cells, in which TG2 expression which results in easily detectable deposition of TG2 into the matrix is under the control of the tet-inducible promoter (13). Using both general and specific inhibitors of

MMPs in these cells, we first demonstrated that MMP-2 and MMP-9, the two major MMPs involved in HS shedding (9,38,39), are required for the deposition of TG2 into the ECM. By protecting or inhibiting the cell surface HS from shedding by treating cells with heparin or the PKC α inhibitor Go6976, TG2 deposition into the matrix was reduced, while PMA, an accelerator for HS shedding, increased the amount of TG2 deposited. Moreover, removal of the HS chains in the TG2 transfected tet-inducible 3T3 cells completely blocked the deposition of TG2 into the matrix. Parallel studies undertaken to measure the amount of syndecan-4 present in the cell matrix after treatment of cells with PMA, PKC α inhibitor Go6976 and the inhibitor of MMP2/9 showed comparable levels of syndecan-4 in the matrix to that found for TG2 when treated with the same key modulators of syndecan shedding. Importantly, knocking down the expression of syndecan-4 expression in these 3T3 cells by siRNA significantly reduced the trafficking of TG2 into the ECM, further confirming the importance of syndecan-4 shedding in matrix TG2 deposition. It is reported that wounding of cells or tissues results in a rapid but transient increase in the TG2 activity found in the matrix surrounding the wound area (22,33). We therefore looked to see if syndecan shedding may also account for this rapid increase in TG2 activity found around the wound area. Our data showed that the increased TG2 activity found around the wound area of TG2-inducible Swiss 3T3 cells could be either partially or totally blocked by agents known to affect syndecan shedding, thus supporting our claims for the importance of syndecan shedding in the trafficking of TG2 into the matrix following its increased expression in cells. Importantly this finding also fits with the suggested role of TG2 as a stress/wound response enzyme (40).

It has been suggested that the mechanism of TG2 secretion from cells may be dependent on conformation and its transition between the closed and open forms (3,41). Using this information and the data obtained for binding of the TG2 mutants to heparin and the importance of syndecan shedding in the trafficking of TG2 into the matrix, one might envisage a mechanism whereby TG2 is first externalised in its closed GTP-bound conformation. It is then retained at the cell surface by its high affinity binding to HS at physiological

ionic strength. Immediate binding to the negatively charged cell surface HS may also be responsible for maintaining the closed conformation of TG2 by sequestration of surrounding Ca^{2+} until the enzyme is translocated into the ECM via syndecan shedding. Once shed and exposed to Ca^{2+} , TG2 will adopt an open conformation and the affinity for HS is significantly reduced, whereas its affinity for FN is increased (**Supplementary Figure 5**) enabling it to bind to and crosslink its matrix substrate proteins such as FN (42) (**Figure 12**). Subsequent oxidation or nitrosylation of the matrix bound enzyme then further modulates its transamidating activity (43,44), such that the enzyme may then act as a novel FN bound cell adhesion protein, either through its interaction with cell surface syndecan-4 or β integrins (19,45).

Strong support for the role of TG2 as a novel cell adhesion protein working via interaction with syndecan-4 comes from the finding that the peptide representing the proposed binding pocket on TG2 for HS (P1 peptide) acted in a comparable manner to TG2 in compensating RGD induced loss of cell adhesion when cells were plated onto FN, using a previously described osteoblast model (5). At concentrations as low as 5-10 $\mu\text{g}/\text{ml}$, compensation of cell adhesion was noted. Moreover, when a $\alpha 5\beta 1$ integrin blocking antibody was used to induce loss of cell adhesion, the P1

peptide, like the full TG2 protein, was able to compensate the loss of adhesion, indicating the potency of this interaction and its ability to mimic TG2 (27). Fluorescence co-staining of F-actin and vinculin further demonstrated the ability of the P1 peptide to restore loss of actin cytoskeleton organization and focal adhesion formation induced by the RGD peptide treatment. Importantly, this compensatory effect of the peptide could be abrogated by pre-treatment of cells with heparinase or treatment of cells with syndecan-4 siRNA, indicating that P1 peptide like TG2 binds to cell surface syndecan-4. These data and the finding that the binding of the P1 peptide to syndecan-4 stimulates activation of PKC α , FAK at Tyr³⁹⁷ and subsequent activation of ERK1/2, confirm the importance of the interaction of TG2 with cell surface syndecan-4 in its role as a cell adhesion protein.

In summary, our findings with HS binding peptide and the discovery of a novel TG2 HS binding site confirm the importance of matrix bound TG2-syndecan-4 interactions in cell adhesion. They also provide a new mechanism for the rapid translocation of TG2 into the ECM involving syndecan shedding. Moreover the demonstration of the potency of the HS binding peptide in modulating cell adhesion may also have future potential applications in regulating cell behaviour in TG2 mediated pathologies.

ACKNOWLEDGEMENTS

Funding for this work was mainly from the EC Marie Curie ITN Project TRACKS (Contract No MRTN-CT-2006-036032) and also from the EC Marie Curie IAPP TRANSCOM (Contract No PIA-GA-2010-251506). Thanks go to Ms Charlotte Bland for the technical support given for fluorescence microscopy.

The authors declare that they have no conflict of interest.

REFERENCES

1. Iismaa, S. E., Mearns, B. M., Lorand, L., and Graham, R. M. (2009) *Physiol. Rev.* **89**, 991-1023
2. Griffin, M., Casadio, R., and Bergamini, C. M. (2002) *Biochem. J.* **368**, 377-396
3. Zemskov, E. A., Mikhailenko, I., Hsia, R. C., Zaritskaya, L., and Belkin, A. M. (2011) *PLoS One* **6**, e19414
4. Gaudry, C. A., Verderio, E., Aeschlimann, D., Cox, A., Smith, C., and Griffin, M. (1999) *J. Biol. Chem.* **274**, 30707-30714
5. Wang, Z., Telci, D., and Griffin, M. (2011) *Exp. Cell Res.* **317**, 367-381
6. Wang, Z., Collighan, R. J., Gross, S. R., Danen, E. H., Orend, G., Telci, D., and Griffin, M. (2010) *J. Biol. Chem.* **285**, 40212-40229
7. Wang, Z., and Griffin, M. (2011) *Amino Acids* [Epub ahead of print]
8. Mahtouk, K., Hose, D., Raynaud, P., Hundemer, M., Jourdan, M., Jourdan, E., Pantesco, V., Baudard, M., De Vos, J., Larroque, M., Moehler, T., Rossi, J. F., Reme, T., Goldschmidt, H., and Klein, B. (2007) *Blood* **109**, 4914-4923
9. Manon-Jensen, T., Itoh, Y., and Couchman, J. R. *Febs. J.* **277**, 3786-3889
10. Tsanou, E., Ioachim, E., Briasoulis, E., Charchanti, A., Damala, K., Karavasilis, V., Pavlidis, N., and Agnantis, N. J. (2004) *J. Exp. Clin. Cancer Res.* **23**, 641-650
11. Fuster, M. M., and Wang, L. *Prog. Mol. Biol. Transl. Sci.* **93**, 179-212
12. Brule, S., Charnaux, N., Sutton, A., Ledoux, D., Chaigneau, T., Saffar, L., and Gattegno, L. (2006) *Glycobiology* **16**, 488-501
13. Verderio, E., Nicholas, B., Gross, S., and Griffin, M. (1998) *Exp. Cell Res.* **239**, 119-138
14. Leblanc, A., Day, N., Menard, A., and Keillor, J. W. (1999) *Protein Expr. Purif.* **17**, 89-95
15. Parsons, M., Keppler, M. D., Kline, A., Messent, A., Humphries, M. J., Gilchrist, R., Hart, I. R., Quittau-Prevostel, C., Hughes, W. E., Parker, P. J., and Ng, T. (2002) *Mol. Cell Biol.* **22**, 5897-5911
16. Gentile, V., Saydak, M., Chiocca, E. A., Akande, O., Birckbichler, P. J., Lee, K. N., Stein, J. P., and Davies, P. J. A. (1991) *J. Biol. Chem.* **266**, 478-483
17. Lee, K. N., Arnold, S. A., Birckbichler, P. J., Patterson, M. K., Jr., Fraij, B. M., Takeuchi, Y., and Carter, H. A. (1993) *Biochim. Biophys. Acta.* **1202**, 1-6
18. Wang, Z., Collighan, R. J., Gross, S. R., Danen, E. H. J., Orend, G., Telci, D., and Griffin, M. (2010) *J. Biol. Chem.* **285**, 40212-40229
19. Telci, D., Wang, Z., Li, X., Verderio, E. A., Humphries, M. J., Baccarini, M., Basaga, H., and Griffin, M. (2008) *J. Biol. Chem.* **283**, 20937-20947
20. Griffin, M., Mongeot, A., Collighan, R., Saint, R. E., Jones, R. A., Coutts, I. G. C., and Rathbone, D. L. (2008) *Bioorg. Med. Chem. Lett.* **18**, 5559-5562
21. Jones, R. A., Nicholas, B., Mian, S., Davies, P. J., and Griffin, M. (1997) *J. Cell Sci.* **110**, 2461-2472
22. Nicholas, B., Smethurst, P., Verderio, E., Jones, R., and Griffin, M. (2003) *Biochem. J.* **371**, 413-422
23. Cardin, A. D., and Weintraub, H. J. R. (1989) *Arteriosclerosis* **9**, 21-32
24. Verderio, E. A. M., Scarpellini, A., and Johnson, T. S. (2009) *Amino Acids* **36**, 671-677

25. Margalit, H., Fischer, N., and Bensasson, S. A. (1993) *J. Biol. Chem.* **268**, 19228-19231
26. Hileman, R. E., Fromm, J. R., Weiler, J. M., and Linhardt, R. J. (1998) *Bioessays* **20**, 156-167
27. Verderio, E. A., Telci, D., Okoye, A., Melino, G., and Griffin, M. (2003) *J Biol Chem* **278**, 42604-42614
28. Hang, J., Zemskov, E. A., Lorand, L., and Belkin, A. M. (2005) *J. Biol. Chem.* **280**, 23675–23683
29. Scarpellini, A., Germack, R., Lortat-Jacob, H., Muramitsu, T., Johnson, T. S., Billett, E., and Verderio, E. A. (2009) *J. Biol. Chem.* **284**, 18411-18423
30. Salo, T., Makela, M., Kylmaniemi, M., Autio-Harmanen, H., and Larjava, H. (1994) *Lab Invest.* **70**, 176-182
31. Fitzgerald, M. L., Wang, Z., Park, P. W., Murphy, G., and Bernfield, M. (2000) *J. Cell Biol.* **148**, 811-824
32. Ritchie, J. P., Ramani, V. C., Ren, Y., Naggi, A., Torri, G., Casu, B., Penco, S., Pisano, C., Carminati, P., Tortoreto, M., Zunino, F., Vlodaysky, I., Sanderson, R. D., and Yang, Y. (2011) *Clin. Cancer Res.* **17**, 1382-1393
33. Pinkas, D. M., Strop, P., Brunger, A. T., and Khosla, C. (2007) *Plos Biology* **5**, 2788-2796
34. Liu, S. P., Cerione, R. A., and Clardy, J. (2002) *Proc. Natl. Acad. Sci. U. S. A.* **99**, 2743-2747
35. Chou, C. Y., Streets, A. J., Watson, P. F., Huang, L., Verderio, E. A., and Johnson, T. S. (2011) *J. Biol. Chem.* **286**, 27825-27835
36. Lidholt, K., Weinke, J. L., Kiser, C. S., Lugemwa, F. N., Bame, K. J., Cheifetz, S., Massague, J., Lindahl, U., and Esko, J. D. (1992) *Proc. Natl. Acad. Sci. U. S. A.* **89**, 2267-2271
37. Alexopoulou, A. N., Mulhaupt, H. A., and Couchman, J. R. (2007) *Int. J. Biochem. Cell Biol.* **39**, 505-528
38. Okina, E., Manon-Jensen, T., Whiteford, J. R., and Couchman, J. R. (2009) *Scand. J. Med. Sci. Sports* **19**, 479-489
39. Su, G., Blaine, S. A., Qiao, D., and Friedl, A. (2008) *Cancer Res.* **68**, 9558-9565
40. Verderio, E. A., Johnson, T., and Griffin, M. (2004) *Amino Acids* **26**, 387-404
41. Johnson, K. A., and Terkeltaub, R. A. (2005) *J. Biol. Chem.* **280**, 15004-15012
42. LeMosy, E. K., Erickson, H. P., Beyer, W. F., Jr., Radek, J. T., Jeong, J. M., Murthy, S. N., and Lorand, L. (1992) *J. Biol. Chem.* **267**, 7880-7885
43. Stamnaes, J., Pinkas, D. M., Fleckenstein, B., Khosla, C., and Sollid, L. M. (2010) *J. Biol. Chem.* **285**, 25402-25409
44. Telci, D., Collighan, R. J., Basaga, H., and Griffin, M. (2009) *J. Biol. Chem.* **284**, 29547-29558
45. Akimov, S. S., Krylov, D., Fleischman, L. F., and Belkin, A. M. (2000) *J. Cell Biol.* **148**, 825-838

FIGURE LEGENDS

Figure 1. 3D structure of TG2 and predicted heparin binding site (A) Surface representation of the crystal structure of TG2 (derived from 1KV3.pdb) with putative HSPG binding sites denoted by coloured shading. The position of the fibronectin binding site (FN) is also given. (B and C) Detailed view of the HS1 and HS2 sites, respectively, showing the juxtaposition of basic residues potentially involved in HSPG binding. (D and E) Predicted binding of a heparin-derived pentasaccharide into the HS1 and HS2 sites, respectively, of TG2. Nitrogen atoms are coloured blue and oxygen atoms red.

Figure 2. Expression and activity of TG2 and site directed TG2 mutants in HEK 293/T17 and NIH 3T3 cells. (A) Representative western blot showing expression levels of wt TG2 and TG2 mutants in HEK 293/T17 cells and (D) NIH 3T3 cells 48 h post-transfection; (B, E) TG2 and mutant TG2 activity in cell lysates of HEK 293/T17 cells and NIH 3T3 cells; (C, F) TG2 and mutant expression levels were normalised to tubulin for equal loading. TG2 and mutant activity in cell lysates of HEK 293/T17 cells (C) and NIH 3T3 cells (F) are normalised for TG2 expression values obtained from Western blotting. Data shown in B-F are from 3 separate experiments.

Figure 3. (A) Differences in the binding strength of TG2 mutants to heparin Sepharose. Cell lysates from HEK293/T17 cells transfected with TG2 and mutants were applied to a heparin Sepharose column (5ml) and eluted with a NaCl gradient as shown. Both flow-through and resulting fractions (1-25 as shown) were assayed for TG2 by Western blotting with CUB7402. (B and C) **The binding specificity of P1 peptide toward syndecan-4.** (B) Solid binding assay was carried on to detect the binding between P1 peptide and recombinant human syndecan-4 or syndecan-2. The presence of the recombinant protein was detected by using anti-his tag antibody as described in the Experimental Procedures. (C) Representative Western blot performed with TG2 tetracycline-inducible Swiss 3T3 cells (tet-) to detect the presence of TG2 in the syndecan-4 immunocomplex in the presence of P1 or P1s peptide as described in the Experimental Procedures.

Figure 4. Effect of P1 peptide on the interaction between TG2 and syndecan-4 and the RGD-induced loss of cell adhesion on FN. (A) **The compensatory effect of P1 peptide on loss of cell adhesion with the RGD peptide.** HOB cells were treated with P1 peptide (0.01 to 200µg/ml) with RAD or RGD peptides on FN. RAD-treated HOB cells were used as the control (the 0 group). Mean percentage value of the control attached and spread cells on FN ± S.D. (control) was set at 100%. (B) **The effect of P1 peptide on the cell adhesion on TG-FN matrix.** FN or TG-FN matrix was prepared as introduced before and HOB cell adhesion assay was performed in the presence of P1 or P1s peptide (100-300µg/ml) on FN or TG-FN matrix as described the Experimental Procedures.

Figure 5. (A) The co-staining of the actin cytoskeleton and vinculin of P1 or P1s-treated HOB cells on FN was undertaken as described in the Experimental Procedures. (B) Shows higher magnification of actin and vinculin staining in the presence of the P1 peptide and RGD with single cell image representing the co-localization of vinculin and actin. Arrows indicate presence of focal adhesion points.

Figure 6. Involvement of the cell surface $\alpha 5\beta 1$ integrin and the importance of the HS chains of syndecan-4 in P1 peptide-regulated cell adhesion. (A) **The involvement of $\alpha 5\beta 1$ integrin.** Cell attachment and spreading was performed in the presence of the $\alpha 5\beta 1$ integrin blocking antibody (20µg/ml) and its isotype control antibody in the presence of P1 or P1s peptide on FN as described in the Experimental Procedures. (B) **Importance of HS chains.** HOB cells pre-treated with heparinase or chondroitinase (15mU/ml) were plated on FN with P1 or P1s peptide (100µg/ml) in the presence of RAD or RGD. Untreated HOB cells represent the control group (CNTL) as described in the Experimental Procedures. Mean percentage value of the control attached and spread cells on FN ± S.D. was set at 100%.

Figure 7. The involvement of syndecan-4 and its downstream signalling molecule PKC α in the P1 peptide mediated RGD-independent cell adhesion. (A) **Requirement of syndecan-4 by the P1 peptide.** Cell adhesion assays using HOB cells treated with syndecan-

4 targeting or NS siRNA on FN in the presence of P1 or P1s control peptide (100ug/ml) was performed as introduced in the Experimental Procedures. Mean percentage value of the control attached and spread cells on FN \pm S.D. was set at 100%. **(B and C) The importance of PKC α in P1 peptide-mediated cell adhesion.** Cell attachment and spreading of HOB cells on FN with RGD or RAD was performed using PKC α inhibitor Go6976 or the GK21 peptide- in the presence of 100ug/ml P1 or P1s peptide as described in the Experimental Procedures. Mean percentage value of the DMSO-treated attached and spread control cells on FN \pm S.D. (control) was set at 100%.

Figure 8. Identification of the intracellular signalling molecules in P1 peptide-mediated signalling transduction. (A-D) Phosphorylation of FAK and ERK1/2 in P1 peptide-mediated signalling transduction. HOB cell adhesion was undertaken with the P1 or P1s peptides (100ug/ml) as described in the Experimental Procedures. P-FAK³⁹⁷ (A) and p-ERK1/2 (C) were detected by Western blotting. Membranes were reprobbed to detect the total FAK or ERK1/2, while α -tubulin was used as the standard for equal loading. Relative amounts of p-397 FAK (B) and p-ERK1/2 (D) compared to total FAK or ERK1/2 was measured by densitometry and normalised to tubulin and then represented as a percentage of that calculated for FN in the presence of RAD. Values are shown as the mean \pm S.D. from 3 separate experiments. **(E-G). Affinity of TG2 and the binding site mutant (D94A, D97A), the N-terminal deletion product of TG2 (Δ 1-15) and the HS2 mutant (K205A, R209A) for binding to FN.** (E) Clarified cell lysates (60 μ g protein) from transiently transfected cells were added to FN-coated plates and the TG2 proteins detected as described in the Materials and Methods. Data shown are normalised for expression of TG2 and its mutants in the different cell lysates using densitometry values from Western blots after normalisation to tubulin. The values represent mean values \pm SD from 3 experiments. **(F and G)** Human recombinant TG2 (2 μ g/ml) was added to microtitre plates previously coated with FN, or the N-terminal 70kDa or 45kDa FN fragments. Prior to addition of the TG2, wells were blocked, washed and then incubated with either the P2 peptide (F) or the scrambled P2 peptide (G, P2s) as described in the Materials and Methods. Data show the mean values \pm S.D. from 3 experiments.

Figure 9. (A and B) Detection of extracellular TG2 in NIH 3T3 cells transfected with wild type TG2 and TG2 mutants and (C-D) presence of extracellular TG2 in CHO K1 cells and the HS deficient CHO-K1 derivative pgsD-677. (A) Cell surface TG2 and mutants were detected by Western blotting after treatment of cells with sulfo-NHS-LC-biotin. Densitometry values (mean value from 2 experiments) for the different TGs are from Western blots normalised for loading and TG2 expression levels as described in **Figure 2**. **(B)** For TG2 and TG2 mutants in the ECM, transfected NIH 3T3 cells were grown for 24 h post transfection in full DMEM medium and for a further 24 h in 1% serum. TG2 antigen in the ECM was detected by Western blotting with Cub7402. The bars in the histogram represents the mean values for matrix TG2 and its mutants as a percentage of the wt TG2 after normalising for the relative expression of TG2 in the cell lysates. Taken from two independent experiments as described in the Experimental Procedures. **(C)** Cell surface TG2 in CHO cells and its HS deficient CHO-K1 derivative was detected after treatment of cells with sulfo-NHS-LC-biotin as described above. **(D)** Relative amounts of cell surface TG2 expressed as a percentage of the wt CHO cells measured by densitometry of the Western blots (mean values from 2 experiments) after normalising to the expression of TG2 as describe in (A) above.

Figure 10. HS shedding and its effects on the trafficking of TG2 into the ECM. General MMP inhibitor GM6001 (GM) (A) or specific MMP inhibitors for MMP-2/ 9, MMP-3 and MMP-8 (10 μ M) (B) were used to treat the TG2 induced (tet-) and non-induced (tet+) 3T3 cells. Cell lysates and matrix fractions after 48 h were western blotted to detect TG2 antigen in the fractions. The bars in the histogram represents the mean values for matrix TG2 represented as a percentage of the non treated control cells after normalising for the relative expression of TG2 in the cell lysates. Taken from two independent experiments as described in the Experimental Procedures. **(C) The effect of HS on TG2 deposition.** Cell lysates and matrix fractions from tet-inducible 3T3 cells induced (tet-) or not induced (tet+) for TG2 were

incubated with PMA (50nM), PKC α inhibitor Go6976 (Go) (5 μ M), heparin (HN) (10 μ g/ml), heparinase (HNase) or chondroitinase (CD) (15mU/ml) were used in Western blotting to detect TG2 and levels (mean of two experiments) expressed as a percentage of the non treated control, calculated as described in (B) above.

Figure 11. (A) Role of syndecan-4 in TG2 deposition into the ECM. Syndecan-4 siRNAs were used to silence syndecan-4 expression in TG2 transfected tet-inducible 3T3 cells prior to detection of TG2 deposition into the ECM in TG2 induced (tet+) and non-induced (tet-) by western blotting. The bars in the histogram represents the mean values for matrix TG2 represented as a percentage of the NS treated control cells after normalising for the relative expression of TG2 in the cell lysates. Taken from two independent experiments as described in the Experimental Procedures. **(B) The presence of shed syndecan-4 in ECM.** Representative dot blot applied to detect the presence of syndecan-4 in the ECM fractions in TG2 transfected tet-inducible 3T3 cells after treatment with PMA(50nM), PKC α inhibitor Go6976(5 μ M) and MMP-2/9 inhibitor(10 μ M), using a specific antibody against the ectodomain of syndecan-4 to detected the syndecan-4 as described in the Experimental Procedures. The histogram represents the mean densitometric values from 2 independent experiments.

Figure 12. The effect of HS in wound –induced TG2 deposition. *In situ* activity of TG2 in TG2 transfected tet-inducible (tet-) 3T3 cells seeded into 8-well chambers detected by incorporation of FITC-cadaverine after different treatments was visualized using fluorescence microscopy as described in the Experimental Procedures. The dotted line marks the edge between the cell area (marked C in the image) and the wound areas (marked W).

Figure 13. Schematic representation of a potential mechanism for translocation of TG2 into the extracellular matrix. Cell surface TG2 in its compact conformation bound to cell surface syndecan-4 is deposited into the ECM by syndecan shedding. This process is regulated by intracellular signalling molecule PKC α , an activator of syndecan-4 shedding. Once shed from the cell surface TG2 takes on its open conformation following increased exposure to Ca²⁺ facilitating both FN binding and matrix deposition and activation of protein crosslinking.

Table 1. Antibodies used in this study

Antigen	Host species	Clone	Company
TG2	Mouse	Monoclonal	Thermo Fisher
p-FAK397	Mouse	Monoclonal	Millipore
Total FAK	Rabbit	Polyclonal	Santa Cruz
p-ERK1/2	Rabbit	Polyclonal	Santa Cruz
Total ERK1/2	Rabbit	Polyclonal	Santa Cruz
Syndecan-4	Rabbit	Polyclonal	Invitrogen
Syndecan-4 ectodomain	Goat	Polyclonal	Santa Cruz
Syndecan-2	Rabbit	Polyclonal	Invitrogen
β 1 Integrin	Rabbit	Polyclonal	Santa Cruz
α -Tubulin	Mouse	Monoclonal	Sigma-Aldrich
Vinculin	Mouse	Monoclonal	Sigma-Aldrich
6 \times His tag	Mouse	Monoclonal	Invitrogen
α 5 β 1 integrin blocking antibody and Isotype control antibody	Mouse	Monoclonal	Biologend
HRP-conjugated anti-mouse secondary	Rabbit		Sigma
HRP-conjugated anti-rabbit secondary	Swine		Dako
TRITC-conjugated anti-mouse secondary	Rabbit		Dako

Table 2. Primers used in this study

Name	TG2 Construct	Primer Sequence
TG2-F	TG2	5' GGTACCATGGCCGAGGAGCTGGTC 3'
FN-F	D94A, D97A	5' GGACAGCCACCGTGGTAGCCCAGCAAGCCTGCACCCTCTCGC 3'
HS1-F	K600A, R601A, K602A	5' GGGGAGCCCAAGCAGGCGGCCGCGCTGGTGGCTGAGGTGTC 3'
HS2-F	K205A, R209A	5' CAACCCCAAGTTCCTGGCGAACGCCGGCGCTGACTGCTCCCG 3'
Δ1-15-F	Δ1-15 TG2	5' GGACGGTACCATGACCAATGGCCGAGACCACCAC 3'
TG2-R	TG2	5' GCGGCCGCTTAGGCGGGGCCAATGATGAC 3'
FN-R	D94A, D97A	5' GCGAGAGGGTGCAGGCTTGCTGGGCTACCACGGTGGCTGTCC 3'
HS1-R	K600A, R601A, K602A	5' GACACCTCAGCCACCAGCGCGGCCGCTGCTTGGGCTCCCC 3'
HS2-R	K205A, R209A	5' CGGGAGCAGTCAGCGCCGGCGTTCGCCAGGAACTTGGGGTTG 3'
Δ 1-15-R	Δ 1-15 TG2	5' GGACGCGGAAGCTTAGGCGGGGCCAATGATGAC 3'

Figure 1

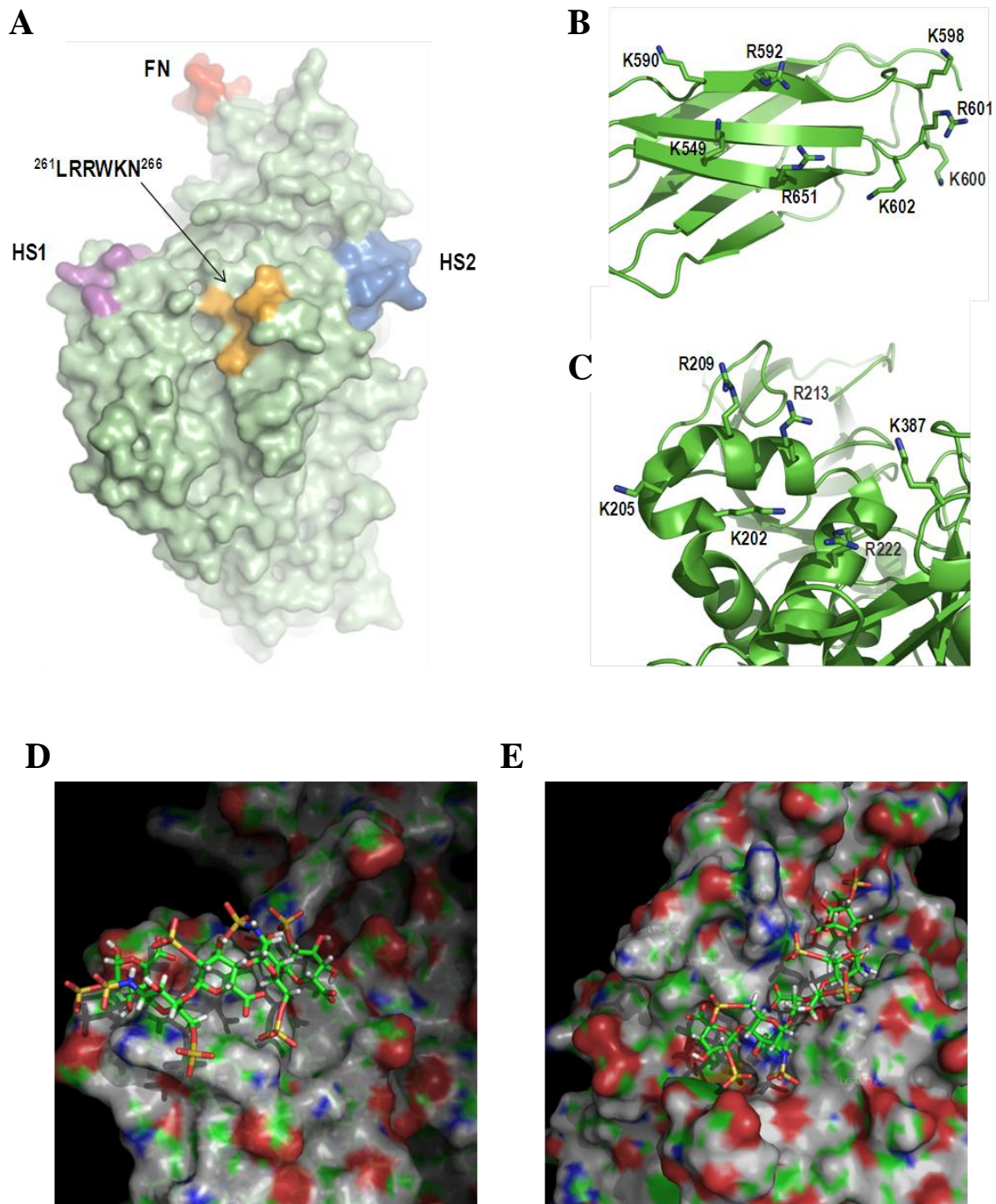


Figure 2

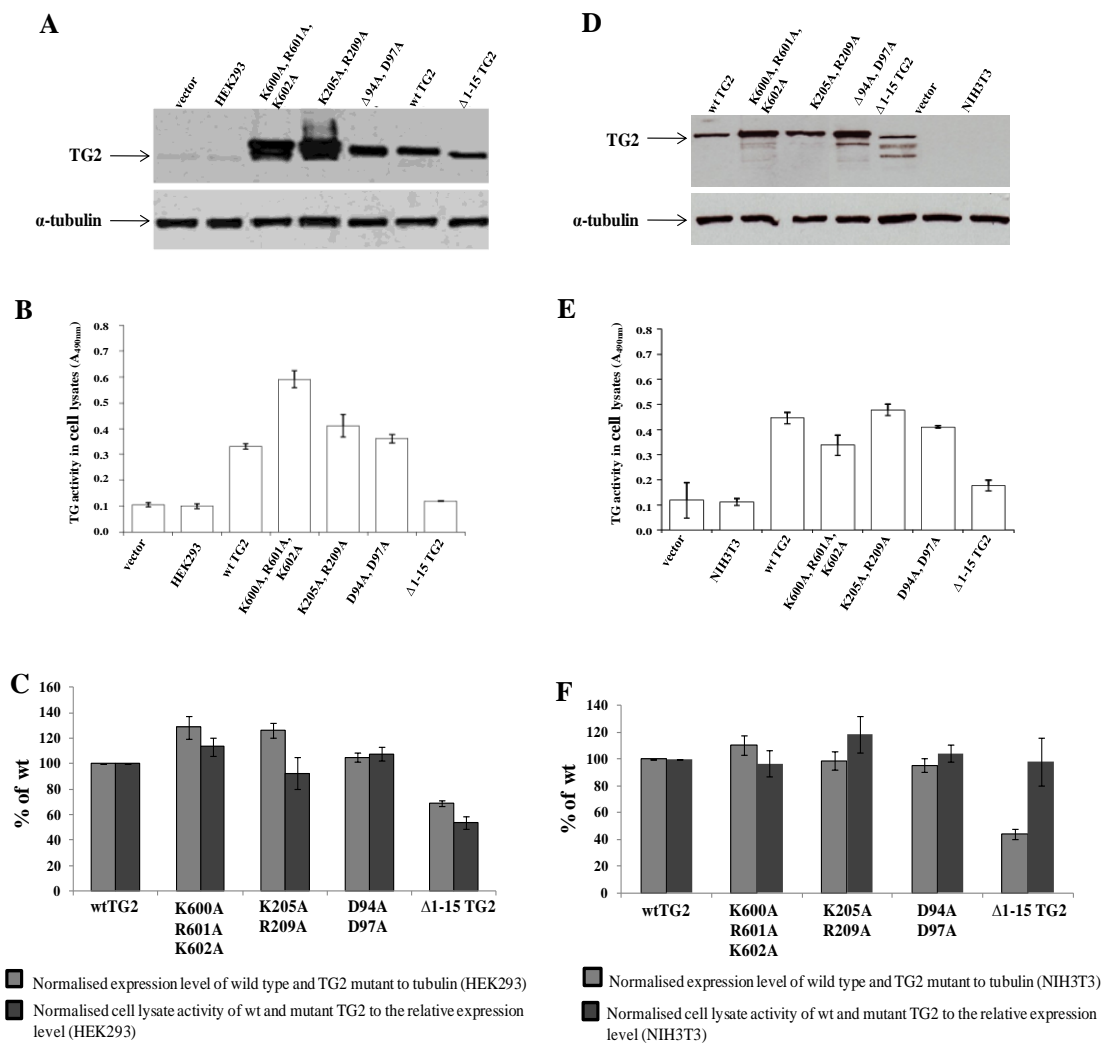


Figure 3

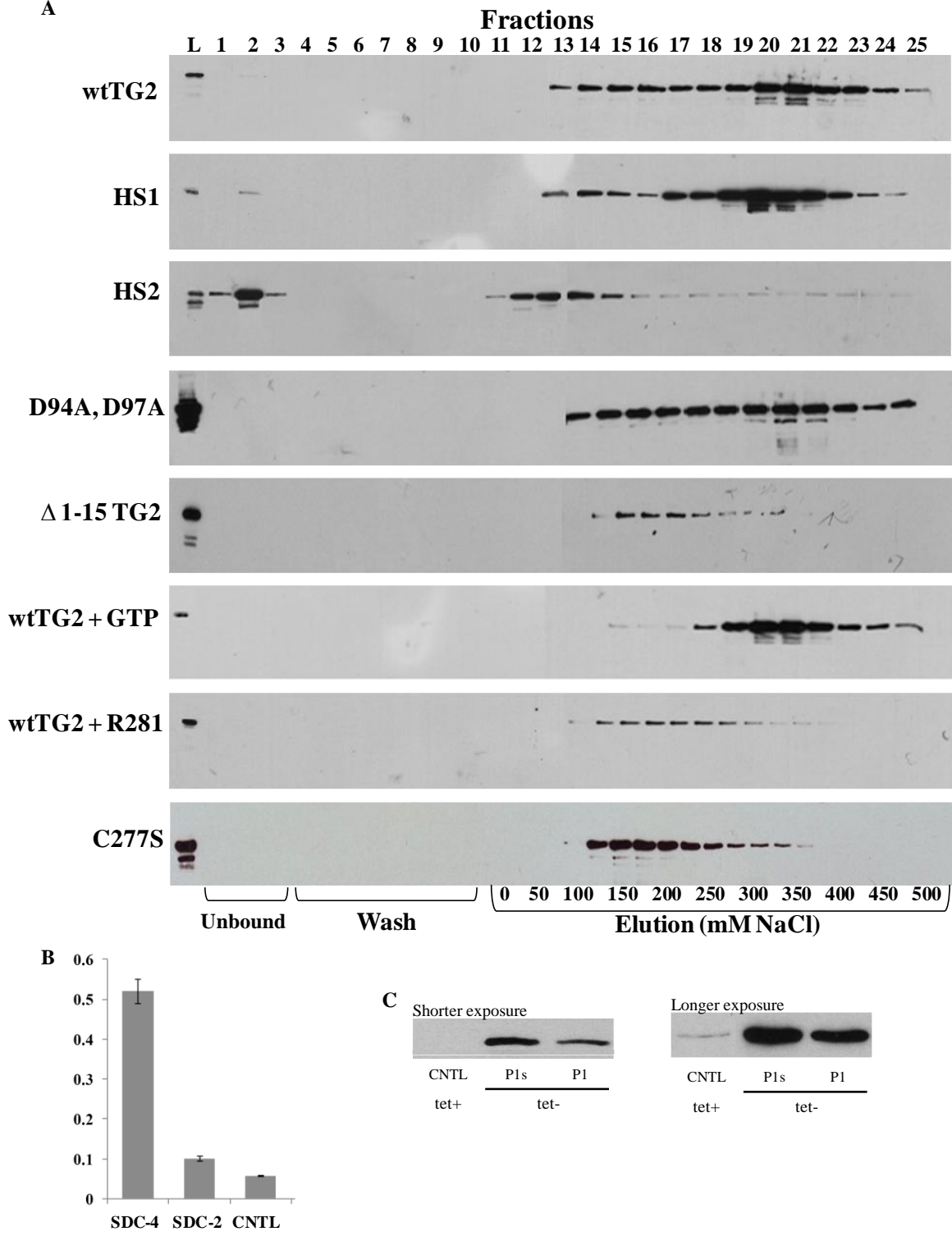


Figure 4

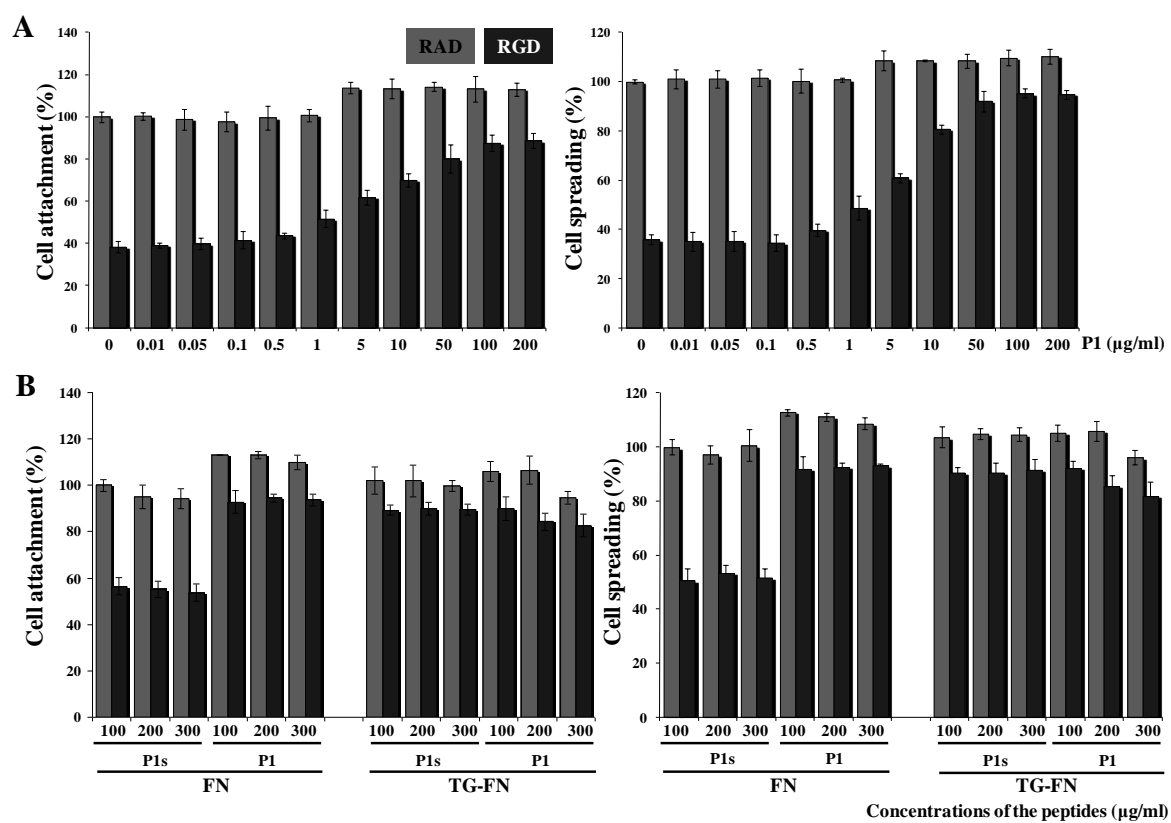


Figure 5

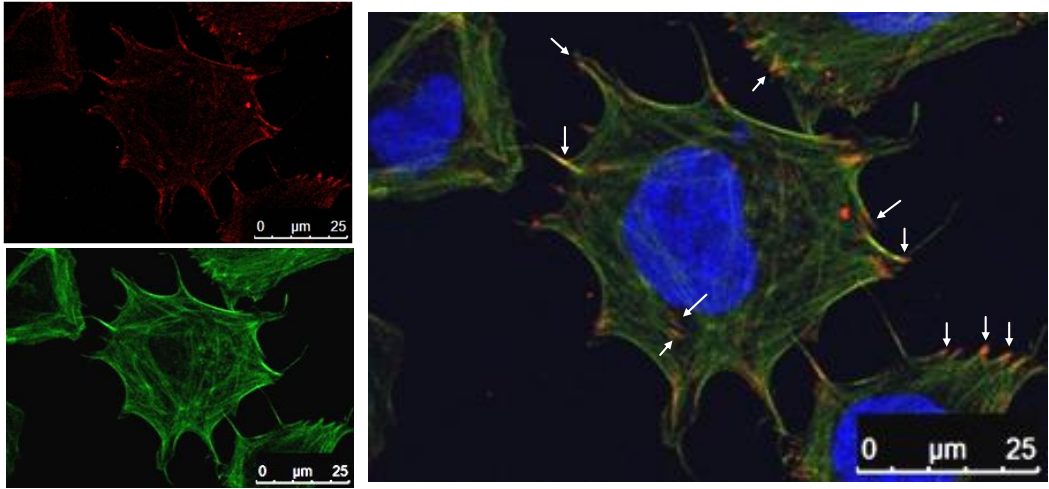
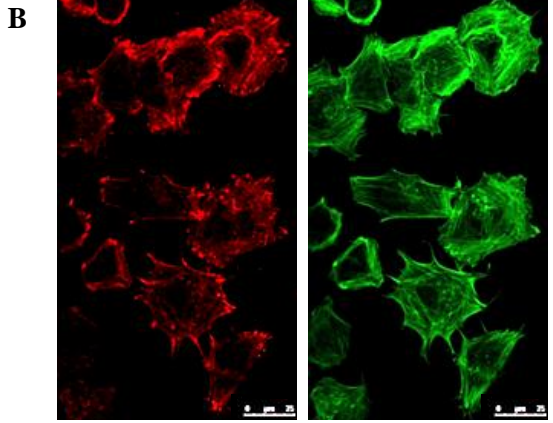
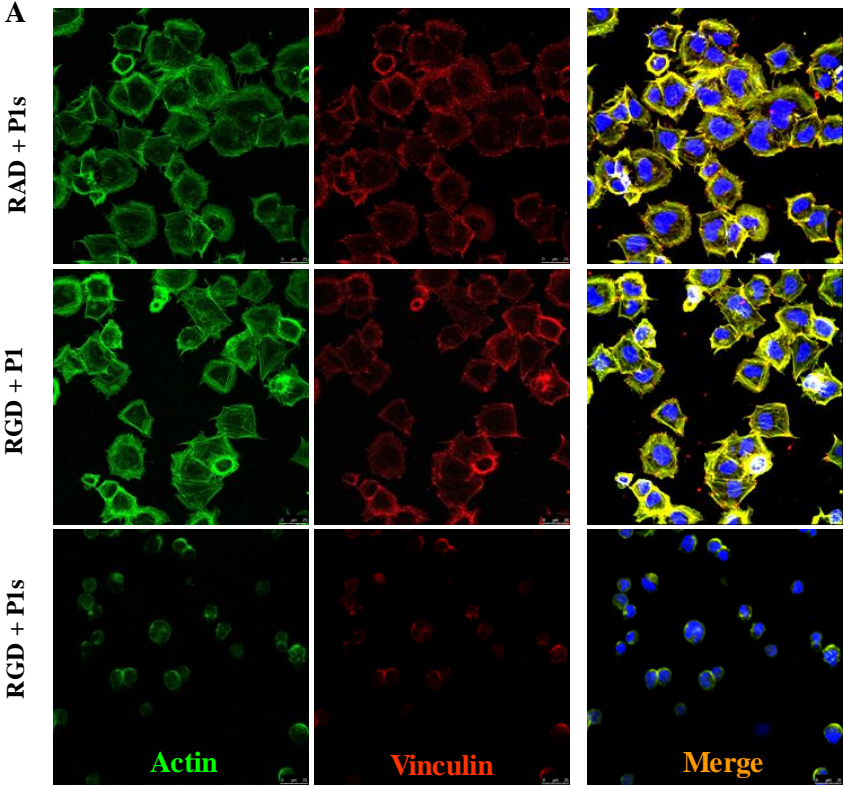


Figure 6

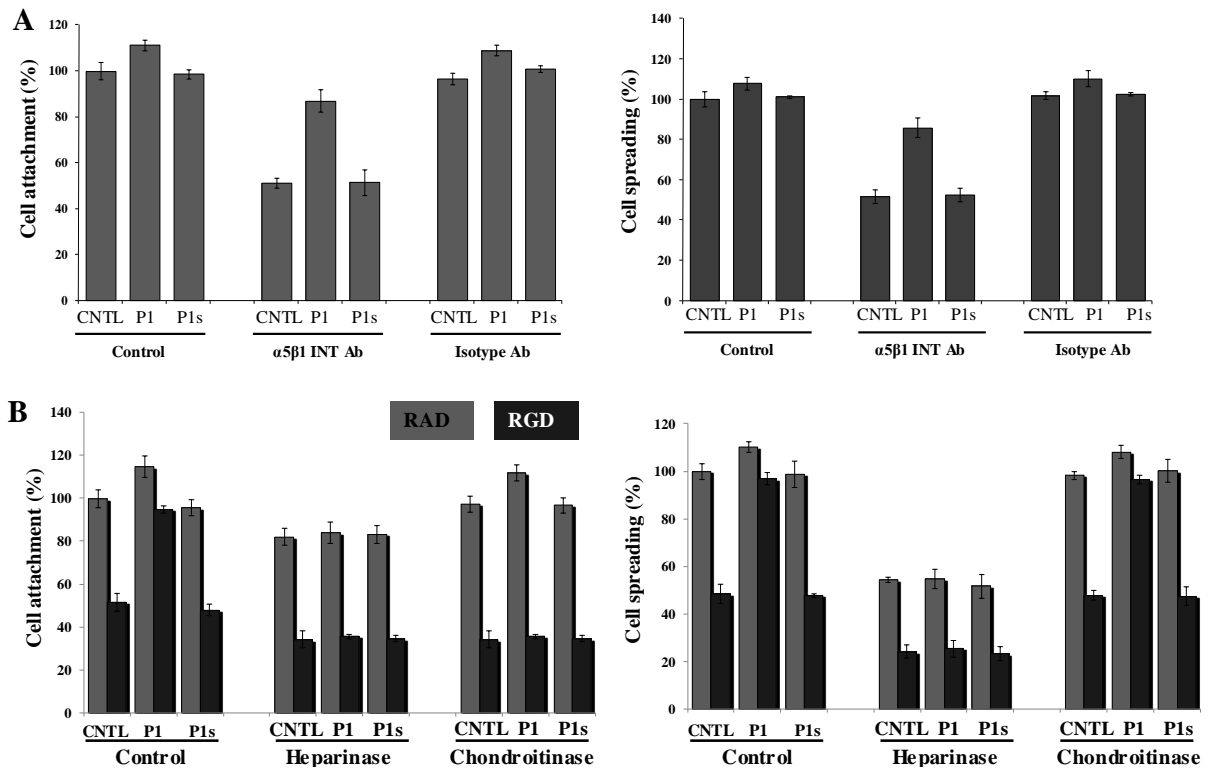


Figure 7

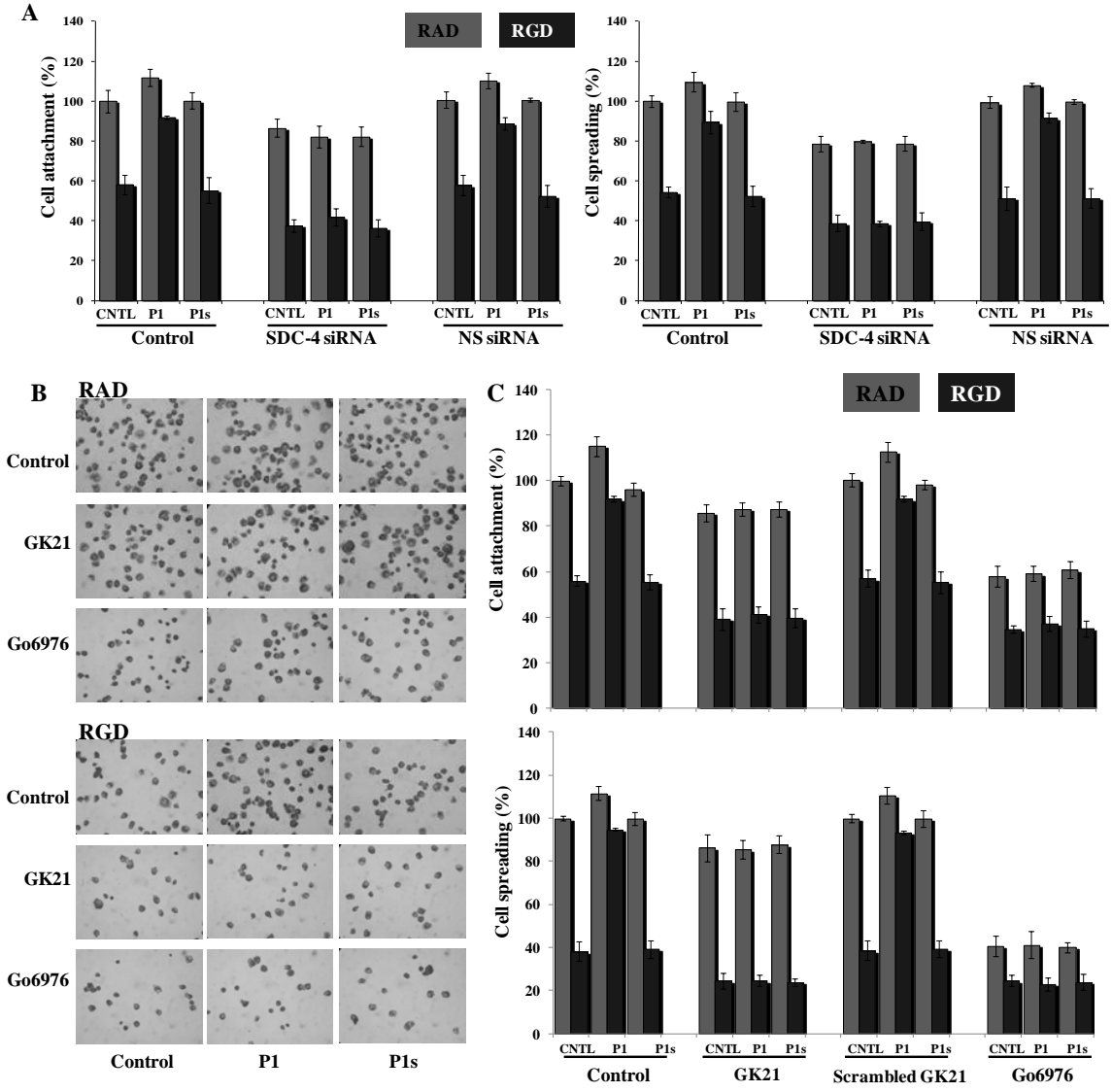


Figure 8

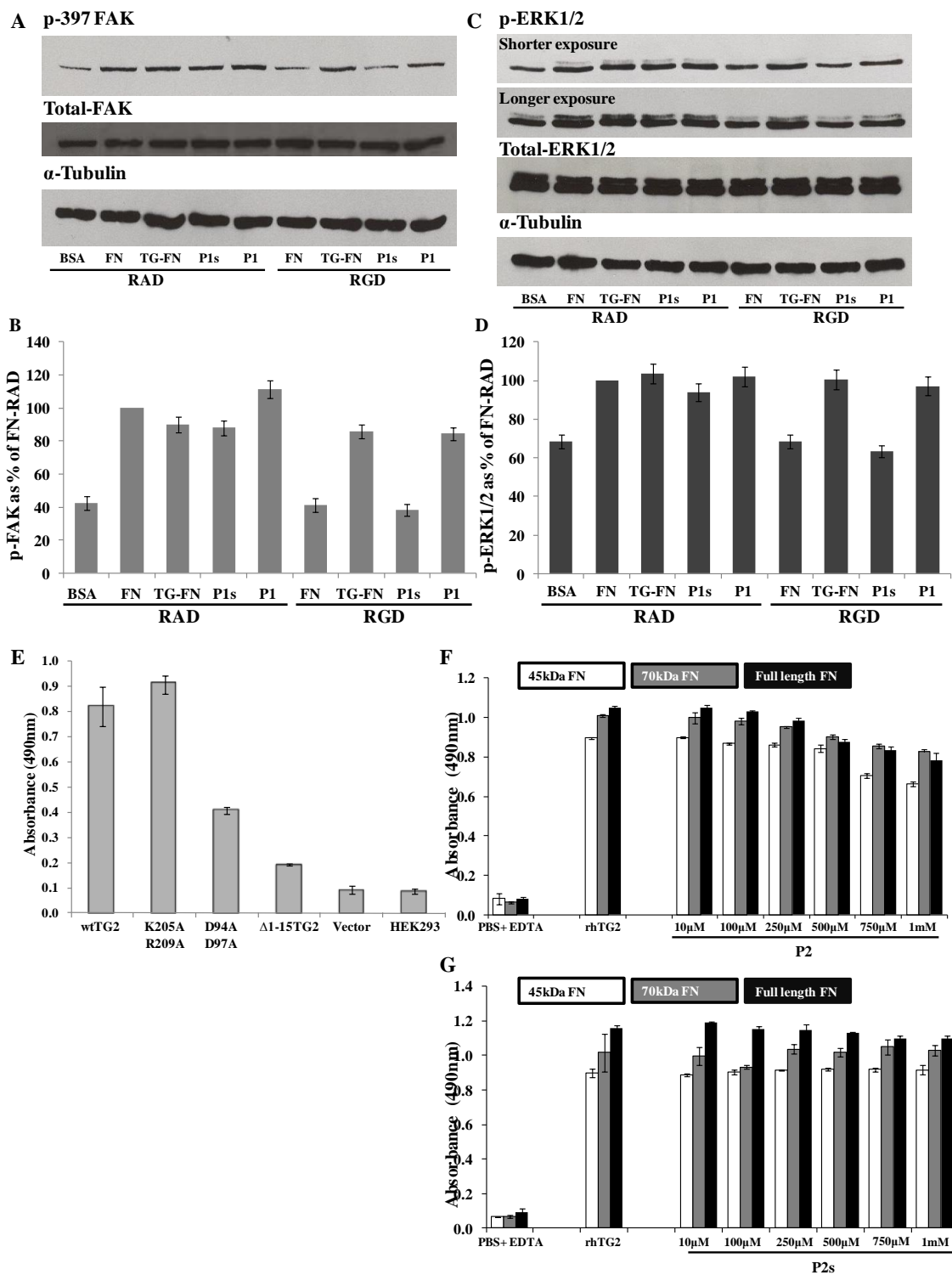


Figure 9

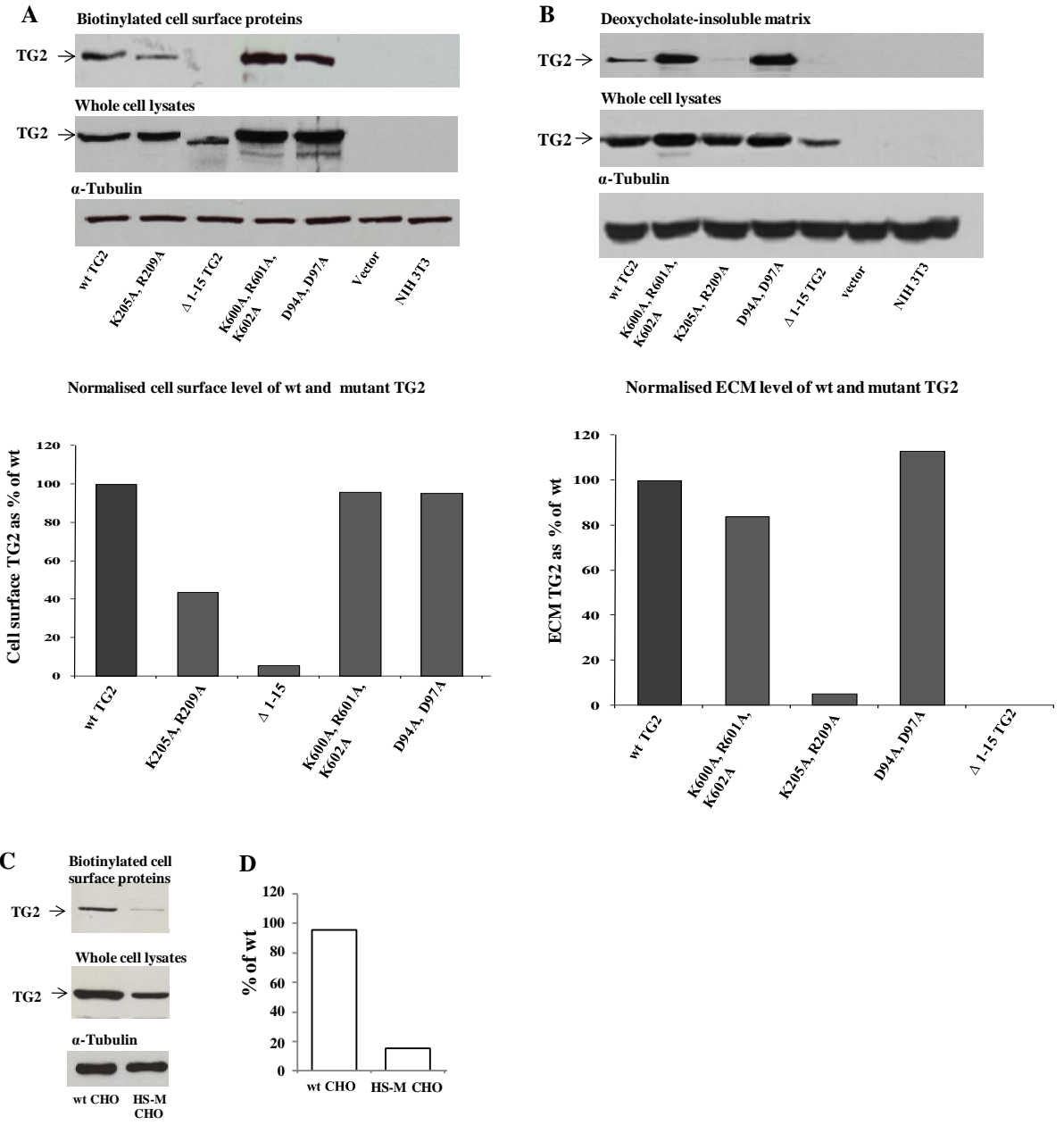


Figure 10

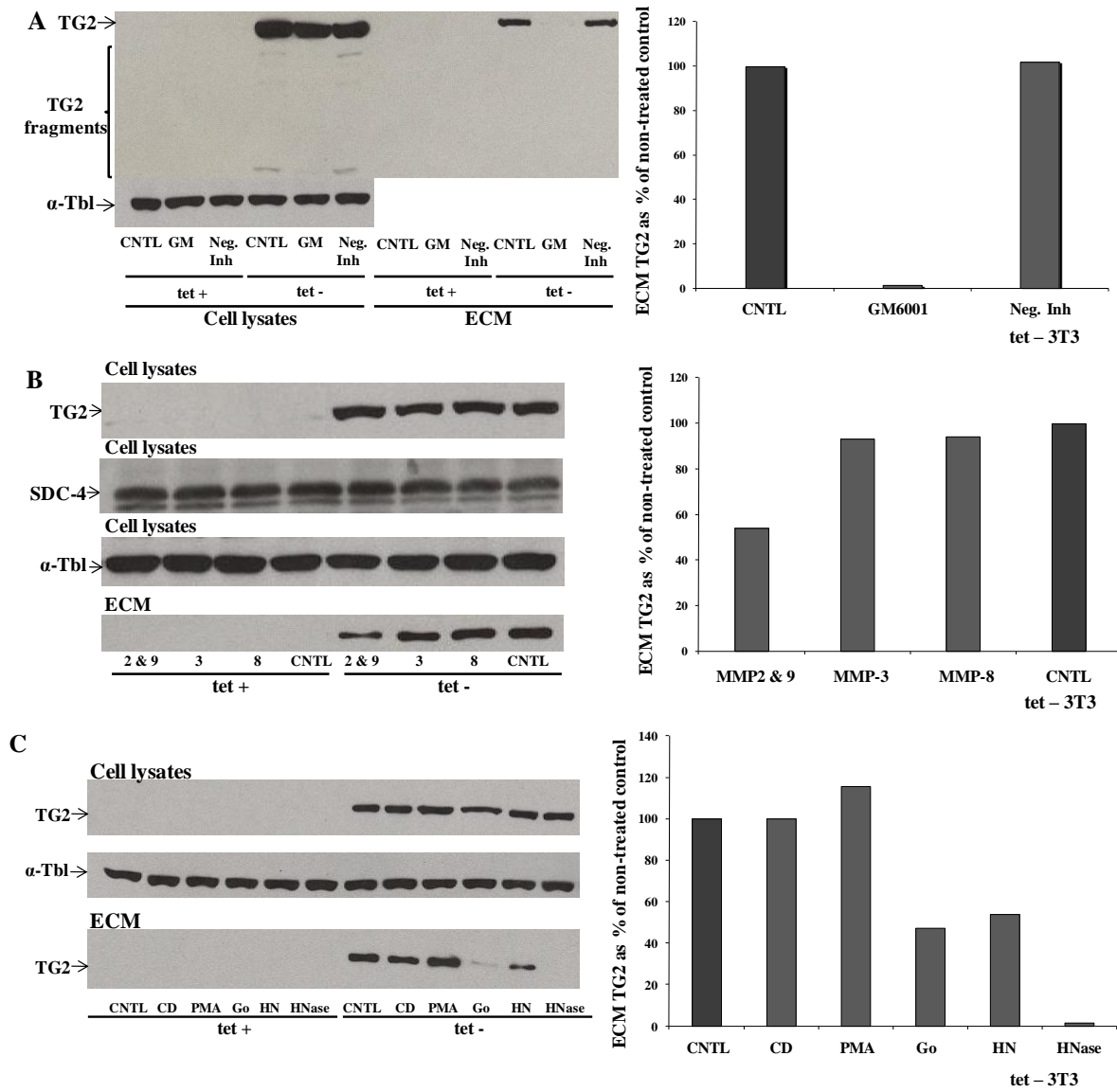


Figure 11

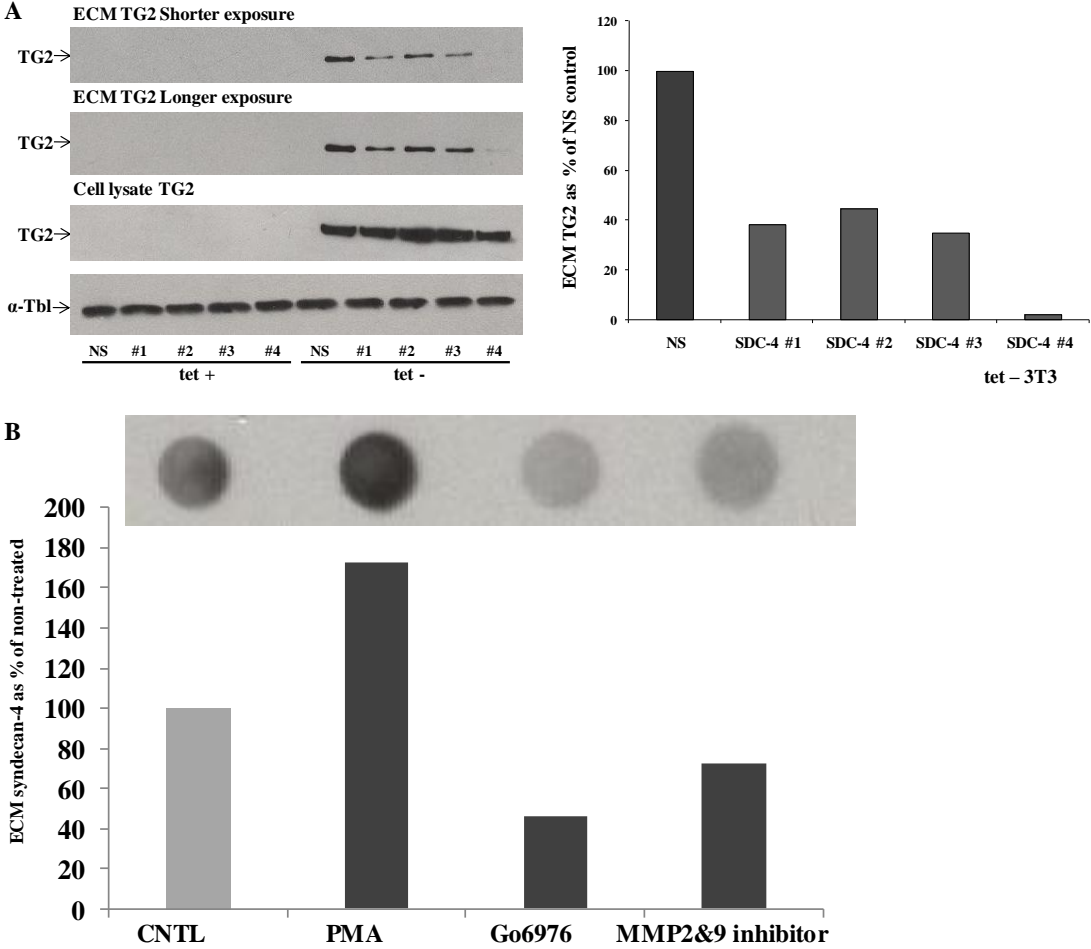


Figure 12

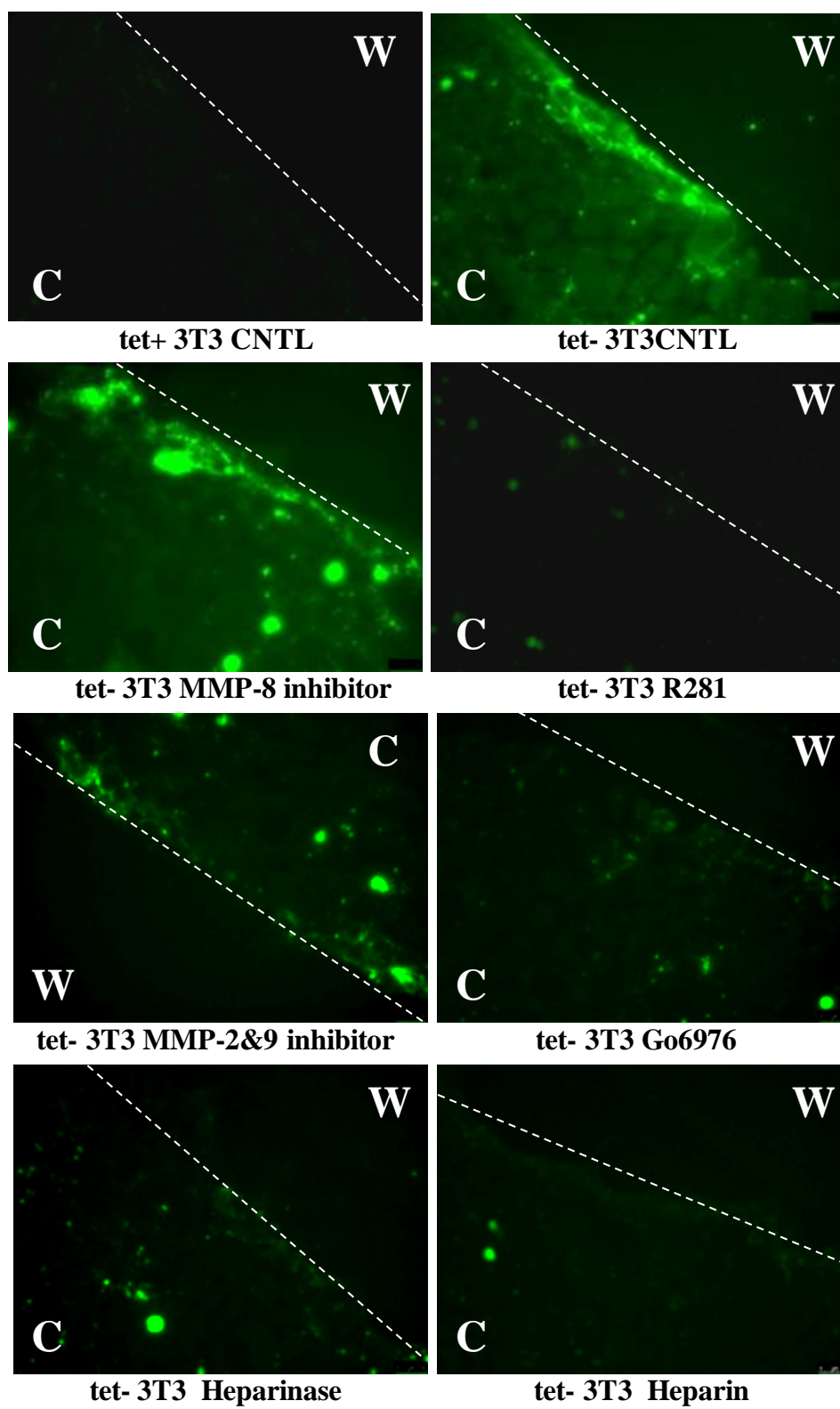


Figure 13

